Tuğba Hazal ALTUNOK

SYNTHESIS, PHYSICOCHEMICAL PROPERTIES AND THEORETICAL MODELLING OF GLUTAMIC ACID AND LYSINE BASED AMPHIPHILIC MOLECULES

M.S.
2014

FATİH UNIVERSITY

The Graduate School of Sciences and Engineering

Master of Science in
Chemistry

SYNTHESIS, PHYSICOCHEMICAL PROPERTIES AND THEORETICAL MODELLING OF GLUTAMIC ACID AND LYSINE BASED AMPHIPHILIC MOLECULES

by

Tuğba Hazal ALTUNOK

January 2014

SYNTHESIS, PHYSICOCHEMICAL PROPERTIES AND THEORETICAL MODELLING OF GLUTAMIC ACID AND LYSINE BASED AMPHIPHILIC MOLECULES

by

Tuğba Hazal ALTUNOK

A thesis submitted to

the Graduate School of Sciences and Engineering

of

Fatih University

in partial fulfillment of the requirements for the degree of

Master of Science

in

Chemistry

January 2014
Istanbul, Turkey

APPROVAL PAGE

This is to certify that I have read this thesis written by Tuğba Hazal ALTUNOK and that in my opinion it is fully adequate, in scope and quality, as a thesis for the degree of Master of Science in Chemistry.

_____
Assist. Prof. Dr. Sedat COŞGUN
Thesis Supervisor

I certify that this thesis satisfies all the requirements as a thesis for the degree of Master of Science in Chemistry.

_____
Assoc. Prof. Dr. Abdülhadi BAYKAL
Head of Department

Examining Committee Members

Assist. Prof. Dr. Sedat COŞGUN _____

Assoc. Prof. Dr. Levent SARI _____

Assist. Prof. Dr. Sevim ÜNÜGÜR ÇELİK _____

It is approved that this thesis has been written in compliance with the formatting rules laid down by the Graduate School of Sciences and Engineering.

_____
Assoc. Prof. Dr. Nurullah ARSLAN
Director

January 2014

SYNTHESIS, PHYSICOCHEMICAL PROPERTIES AND THEORETICAL MODELLING OF GLUTAMIC ACID AND LYSINE BASED AMPHIPHILIC MOLECULES

Tuğba Hazal ALTUNOK

M.S. Thesis – Chemistry
January 2014

Thesis Supervisor: Assist. Prof. Dr. Sedat COŞGUN

ABSTRACT

In this master thesis amino acid based double chained cationic amphiphilic molecules have been studied including lysine and glutamic acid. Two chains on the amphiphiles were attached by forming amide and ester bonds and the alpha amino group was choosen as the cationic part. By using different types of amino acids and bond types, both difference of glutamic acid and lysine, effect of amide bond and ester bond was tried to be determined. In order to make this some of the physical techniques were used such as POM, SEM, etc.

Another subject of this master thesis is to compare experimental and theoretical results of the self-assembly behavior of the amphiphiles.

Keywords: Double-chained surfactants, Cationic surfactants, Self-Assembly behavior, Packing parameter.

GLUTAMİK ASİT VE LİZİN ESASLI AMFİFİLİK MOLEKÜLLERİN SENTEZİ, FİZİKOKİMYASAL ÖZELLİKLERİ VE TEORİK MODELLEMESİ

Tuğba Hazal ALTUNOK

Yüksek Lisans Tezi – Kimya
Ocak 2014

Tez Danışmanı: Yrd. Doç. Dr. Sedat COŞGUN

ÖZ

Bu yüksek lisans tez çalışmasında, glutamik asit ve lizin içeren amino asit bazlı, iki zincirli, katyonik amfifilik moleküller çalışılmıştır. Amfifiller üzerindeki iki zincir amit ve ester bağları ile bağlanmış ve katyonik kısım alfa amino grubu olarak seçilmiştir. Farklı amino asitlerin ve bağ türlerinin kullanımı ile, glutamic asit ve lizin, amit bağı ile ester bağı arasındaki fark belirlenmeye çalışılmış, bu amaçla POM, SEM gibi bazı fiziksel tekniklerden yararlanılmıştır.

Master tezinin bir diğer amacı ise amfifillerin kendiliğinden yığılma davranışının teorik ve deneysel sonuçlarının kıyaslanmasıdır.

Anahtar Kelimeler: İki zincirli surfaktanlar, Katyonik surfaktanlar, Moleküllerin agregasyon davranışı, Packing parametre.

To my family

ACKNOWLEDGEDMENTS

At the end of my thesis I would like to thank all those people who made this thesis possible and an unforgettable experience for me.

Firstly, I would like to express my most sincere gratitude to my thesis supervisor to Assist. Prof. Dr. Sedat COŞGUN for his guidance and patience.

Besides my advisor, I am also grateful to Zafer SÖYLER and my lab mate Salif DIATTA for their enormous help and great friendship.

Additionally, I would like to thank Assoc. Prof. Dr. Ahmet ALTUN, Assoc. Prof. Dr. Levent SARI and Tayyibe BARDAKÇI to share their knowledge with me.

I am very fortunate to have had the opportunity to be friends Boran ULUCA, Sevda AKAY, Merve ALTIKARDEŞ, Berna BÜYÜK, Kübra Zeynep ASLIYÜKSEK and my friends at school who always have accompanied me in my hard and good times in addition to their scientific discussions.

Lastly, my deep thanks go to my family for their love, encouragement, support, care and patience. This dissertation is dedicated to them.

TABLE OF CONTENTS

LIST OF TABLES

TABLE

LIST OF FIGURES

FIGURE

LIST OF SYMBOLS AND ABBREVIATIONS

SYMBOL/ABBREVIATION

Asn	Asparagine
BOC	tert-Butyloxycarbonyl
BOP	Benzotriazole-1-yl-oxy-tris-(dimethylamino)-phosphonium Hexafluorophosphate
C12GluDiamide	1,5-bis(dodecylamino)-1,5-dioxopentan-2-aminium
C12GluDiester	1,5-bis(dodecyloxy)-1,5-dioxopentan-2-aminium
C12GluAmidoester	5-(dodecylamino)-1-(dodecyloxy)-1,5-dioxopentan-2-aminium
C12GluT	Glutamic Acid/Dodecyl Amide Salt
C12GluN	2-ammonio-5-(dodecylamino)-5-oxopentanoate
C12LysT	Lysine/Lauric Acid Salt
DDS	Drug Delivery System
Et3N	Triethylamine
FT-IR	Fouirer Transform Infrared Spectroscopy
HCl	Hydrogen chloride
HF	Hartree–Fock
HLB	Hydrophile–Lipophile Balance
HMPT	Hexamethylphosphoramide
Mes	Mesitylene
MP	Melting Point
NaCl	Sodium Chloride
NaOH	Sodium Hydroxide
NMR	Nuclear magnetic resonance
P	Packing Parameter
POM	Polarized Optical Microscopy
Ppm	Parts per million
SEM	Scanning electron microscop

CHAPTER 1

INTRODUCTION

1.1 AMPHIPHILES & SURFACTANTS

In recent years, amphiphilic molecules have become increasingly important for industrial and academic research groups [1]. The properties and applications of amphiphiles are fairly common. Because of their potential to bridge from the molecular scale to the nanoscale, amphiphiles have extraordinary value. The most important examples of amphiphiles are surfactants which consumed in large quantities everyday on a worldwide scale, due to their wide-ranging applications in detergent, pharmaceutical industries, food technology, etc [2, 3].

Amphiphile is a word coined by Paul Winsor 60 years ago from combination of two Greek roots: amphi and philos. Amphi expresses double as in amphitheater or amphibian and philos means affinity as in philosopher or hydrophilic. An amphiphilic molecule consists of two parts: polar group and apolar part. The polar part which includes functional groups such as alcohol, thiol, ester, amide, etc… is also called hydrophilic part or hydrophile. The apolar portion is an hydrocarbon chain generally and this portion is called hydrophobe or lipophile [4].

In English the term surfactant (surface-active-agent) may be defined as a material that can reduce the surface tension of water when present at a low concentration in a system. Surfactant molecules are generally organic compounds that are amphiphilic and they contain both hydrophobic parts and hydrophilic parts like in amphiphilic molecules, but some amphiphiles do not display superficial or interfacial activity, if the amphiphilic molecule is too hydrophobic or too hydrophilic [5]. Amphiphiles display other features than tension lowering and they are often labeled according to their main characteristic such as: detergent, soap, wetting agent, emulsifier, etc. and sometimes

they are named by the structure they are able to construct, i.e. liposome, vesicle, gel or membrane [4].

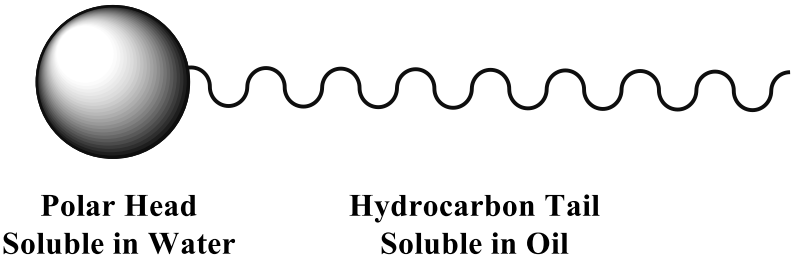

Figure 1.1 Basic structure of a surfactant molecule.

1.1.1 Classification of Surfactants

The most useful chemical classification of surface-active agents is based on the nature of the hydrophile, with subgroups based on the nature of tail. The four basic classes of surfactants are defined as follows:

1. Anionic—the hydrophile bears a negative charge, such as carboxyl, sulfate or phosphate.

2. Cationic—the hydrophile is a positively charged group, as for example, the quaternary ammonium halides.

3. Nonionic—the hydrophile has no charge, but derives its water solubility from highly polar groups such as polyoxyethylene.

4. Amphoteric (and zwitterionic)—the molecule contains both a negative charge and a positive charge, such as the sulfobetaines [6].

1.1.1.1 Cationic Surfactants

Cationic surfactants behave as good antimicrobial agents and have been used as disinfectants in hospital and in the food industry depend on their two important features: easily absorbance at solid/liquid interphases and interaction with the cellular

membranes of microorganisms [7, 8]. Cationic amphiphiles have great potential in new therapeutic biomedical applications as antimicrobial and antifungal agents, and can also be used in gene therapy, as vehicles for certain drugs and as modifiers of the physicochemical and biological properties of biomaterials [9-14]. Especially interesting in medicine and pharmacology are the synthesis and characterization of biodegradable cationic amphiphiles with low cytotoxicity [15].

1.1.2 Amino Acid Based Surfactants

Surfactants are widely used excipients in the pharmaceutical industry [16]. Their surface and interface activities in systems have been the subject of intense researchs. Amino acid based surfactants are an important class of natural surface-active molecules that usually have biocompatible properties and multifunctional capabilities, particularly in the field of drug delivery vehicles [17].

The extensive use of surfactants in both hausehold and industrial products requires the search for ever “greener” amphiphiles. The synthesis of amino acid based surfactants that mimic naturally occuring lipoaminoacids has provided molecules with lower irritancy and toxicity for living organisms as well as higher biodegradability when compared to conventional surfactants. It has also been observed that these surfactants have antimicrobial and antiviral activity [18].

Interest in amino acid based surfactants traces back to 1909 when for the first time was obtained N-acyl glycine and N-acyl alanine. Since then, amino acid based surfactants have been the subject of intense studies, because of their huge potential applications in pharmaceutical, cosmetic, household and food products. Currently these types of surfactants are commercially applied in a lot of esters and amides have excellent emulsifying and strong antimicrobial properties, which make them a good alternative as food additives [19].

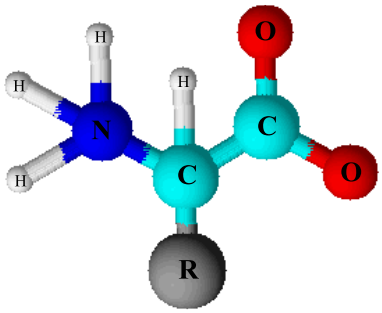

Figure 1.2 Basic structure of an amino acid.

Theoretically the hydrophobic group is bonded to the amino acids either at the amine moiety or at the carboxylic moiety. So that, four main synthesis paths are deduced based on this approach, which are described in Figure 1.3. By modifying the type of bond the characteristics of the resulting surfactants will be influenced [20].

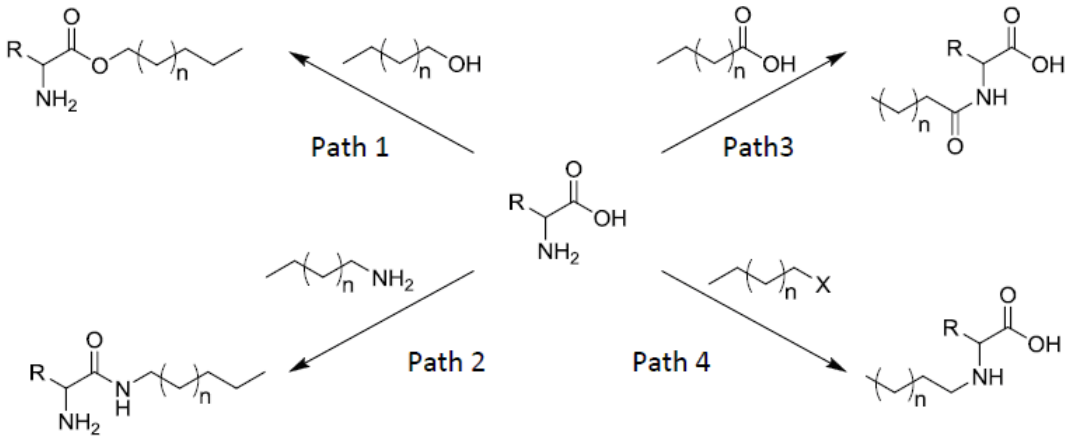

Figure 1.3 Fundamental synthesis paths of amino acid based surfactants [20].

In path 1, an amphiphilic esteramine is obtained by the reaction of fatty alcohol and amino acid. Such reaction is an esterification, which is obtained by refluxing the amino acid and fatty alcohol in the presence of acidic catalyst and dehydrating agent. Ordinarily concentrated sulfuric acid is used as both catalyst and dehydrating agent.

In path 2, an amphiphilic amidoamine is achieved by the reaction of amino acid with an alkyl amine. Generally the acid is activated and then reacted with the amine.

In path 3, the amine group of amino acid reacts with fatty acid and, generally under the form of an acyl chloride, and an amidoacid is obtained.

In path 4, in order to produce a long-chain alkyl amino acid, the amine group is reacted with an alkyl halogen [20].

Lipoamino acids are easy to design and synthesize. The presence of one carboxylate and two amino moieties in lysine and two carboxylates and one amino moiety in glutamic acid makes them possible to design various types of surfactants of different ionic character (anionic, cationic, nonionic and amphoteric derivatives) by introducing hydrophobic groups (fatty acid/fatty amine or fatty alcohol) into the molecule [21]. Because of that, these amino acids constitute a prime raw materials for the preparation of biodegradable and biocompatible cationic surfactants [15].

1.1.3 Surface Tension

The surface tension is the factor representing the uncompensated intermolecular forces acting in the bulk phase (Fig.1.4) In the bulk, each molecule is surrounded by identical neighbours acting at any point in the bulk is the same.

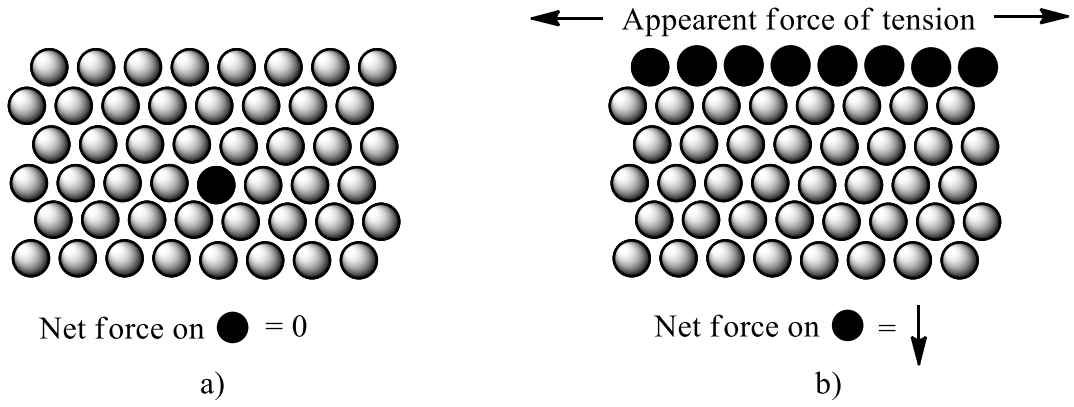

Figure 1.4 Atoms at interfaces, the origin of interfacial energy: (a) bulk atom or molecules; (b) surface atoms or molecules [22].

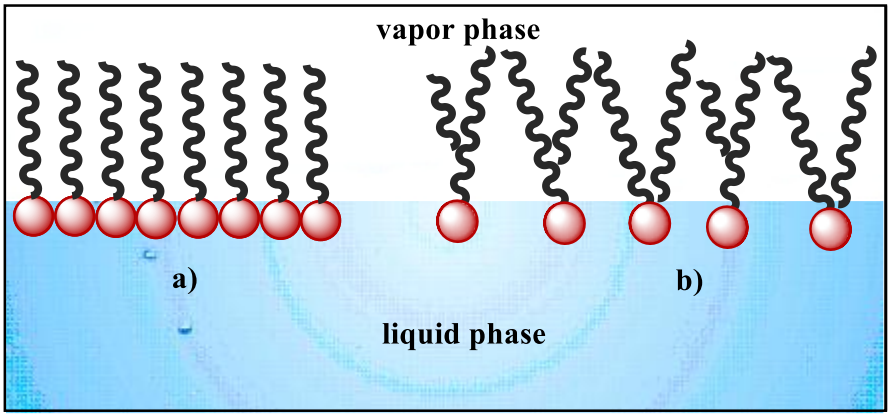

Figure 1.5 The role of surfactant structure and packing in the determination of packing efficiency and surface tension: (a) straight-chain hydrophobes, closest packing and maximum effectiveness; (b) branched, unsymmetric, substituted, and other types of tails reduce packing efficiency [22].

1.1.4 Self-Assembly Behavior of Surfactants

The self-assembly of the surfactants in solutions has been widely investigated both experimentally and theoretically, because of the advantages of the resulting multimolecular aggregates in practical applications [23]. The main abilitiy of the surfactant molecules is to change the energy of interfaces. They aid connected to a hydrophobic alkyl chain. This antagonism is responsible for the characteristic behavior of surfactants in contact with solvents. Surfactant molecules have tendency to minimize the water-alkyl and to maximize the water-head group interfaces. This is responsible for the well-documented self-assembly processes leading to micelles, lytropic phases and emulsions, depending on the concentration and the presence of the additives [2].

The structure of aggregates influences the properties of surfactant solutions, such as their solubilization capacity for hydrophobic substances or their viscous properties, and the performance of surfactants in various applications. To select molecules that would yield desired structures such as micelle, hexagonal, lamellar, etc., it is necessary to know the effect of the molecular structure of the surfactant on the shape and size of the resulting aggregates [23].

1.2 HYDROPHILE-LIPOPHILE BALANCE

For a while, a goal of surfactant related research has been to find a quantitative way to relate the chemical structure of surfactant molecules directly to their physicochemical activity in use. One of the earliest attempts came from the cosmetics industry to correlate surface activity and chemical structure and this is known as the ‘‘hydrophile–lipophile balance’’ (HLB) system which was invented in 1949 by William Griffin. The HLB system relates the molecular composition of a surfactant and its properties. Although it is not a quantitative panacea for designing surfactants, it continues to be an important tool in the surfactant formulation technology [6, 24]. The method works as follows:

$$HLB = 20.Mh/M \tag{1.1}$$

Where *Mh* is the molecular mass of the hydrophilic portion of the molecule, *M* is the molecular mass of the whole molecule. If the HLB value is smaller than 10, the molecule is lipid soluble and if the HLB is bigger than 10, the molecule is water soluble.

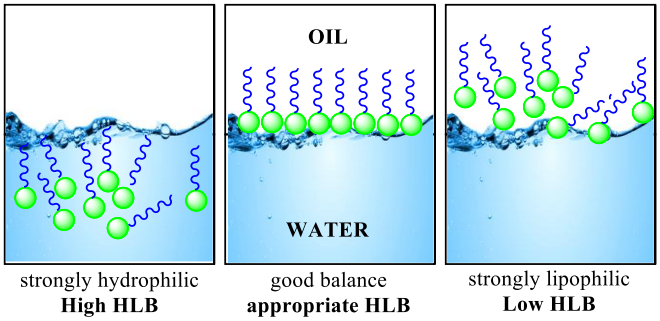

Figure 1.6 HLB and emulsifiers in water/oil.

In recent years, attempts have been made to use more theoretically ‘‘satisfying’’ tools such as the concepts of cohesive energy densities and molecular geometry to correlate such relationships as chemical structure of surfactant, the nature of the solvent, and surfactant activity on atomic and molecular levels [6].

1.3 PACKING PARAMETER

Tanford and Israelachvili, Mitchell and Ninham pioneered two of the most important ideas to answer how the molecular structure of the surfactant controls the shape and size of the resulting aggregate, more than 35 years ago. In order to formulate a quantitative expression for the standard free energy change on aggregation, Tanford proposed the concept of opposing forces. He was able to explain why surfactant aggregates form in aqueous solutions, why they grow and do not keep growing but are finite in size and why they assume a given shape, using free energy expression and the geometrical relations for aggregates. Israelachvili, Mitchell and Ninham proposed the concept of molecular packing parameter and demonstrated how aggregation type can be predicted from a combination of molecular packing considerations and general thermodynamic principles [23].

In order to explain the synergy in the surface aggregation, packing parameter is used [25]. This parameter is defined as $P = V/a_0l$, where v and l are volume and chain lenght of the hydrophobic group, respectively, and a_0 is the cross-sectional area of the head group dictated by the electrostatic repulsion between adjacent headgroups can increase the packing factor (P). The pH, temperature and salinity can all change the electrostatic repulsion and thus the aggregation morphology [26]. As can be seen on the table the critical packing parameter is 1/3 for the sphere-to-cylinder transition, 1/2 for the cylinder-to-bilayer and vesicle transition, 1 for the transition to lamellar and after 1 for the reversed micelle and hexagonal.

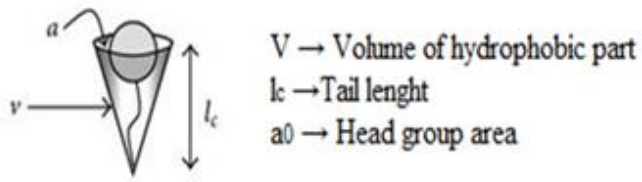

Figure 1.7 Illustration of V, l_c and a_o.

Table 1.1 Molecular P of Israelachvili and corresponding surfactant shape.

Packing parameter	Surfactant Shape			Aggregation behavior	
P < ½	Cone			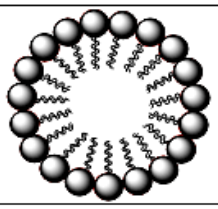	-Micelles -Hexagonal I
½ < P < 1	Truncated Cone			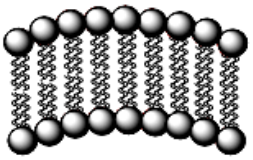	-Flexible Lamellar =vesicles
P ≈ 1	Cylinder	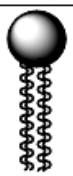		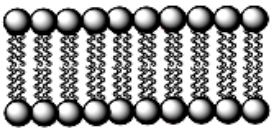	-Lamellar -Cubic
P > 1	Inverted Truncated Cone	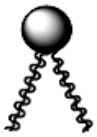		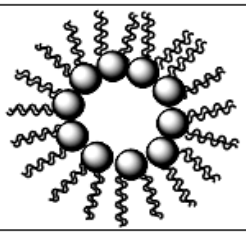	-Reversed Micelles -Hexagonal II

1.4 DRUG DELİVERY SYSTEMS

The best part of drugs have undesirable risk of side effects besides providing the desired therapeutic effects [27]. In order to minimize the side effects and bring the drug concentration to a specific level and maintain it at that level for a specified amount of time, drug delivery systems (DDS) are produced. For the design of successful drug formulation, stability and solubility are two key physicochemical properties that must be considered [28]. Advances in DDS have improved pharmacokinetics and biodistribution of drugs that suffer from poor stability, poor solubility and toxicity. These systems (liposomes, dendrimers, micelles, etc.) make easier encapsulation targeting and release of drugs [29].

The use of liposomes in drug delivery has advantages and disadvantages. The amphiphilic character of the liposomes enables solubilization or encapsulation of both hydrophobic and hydrophilic drugs. Along with their good solubilization power, a

relatively easy preparation and a rich selection of physicochemical properties have made liposomes attractive drug delivery systems. Biological stability includes control over the rate of clearance of liposomes from the circulatory system, if the drug has been administered locally. Biological stability also includes retention of the drug by the carrier en route to its destination. For example, blood proteins were found to remove phospholipid molecules rapidly from the bilayer, leading to a disruption of the liposomes and therefore drug loss before the carriers reached their target destination [30].

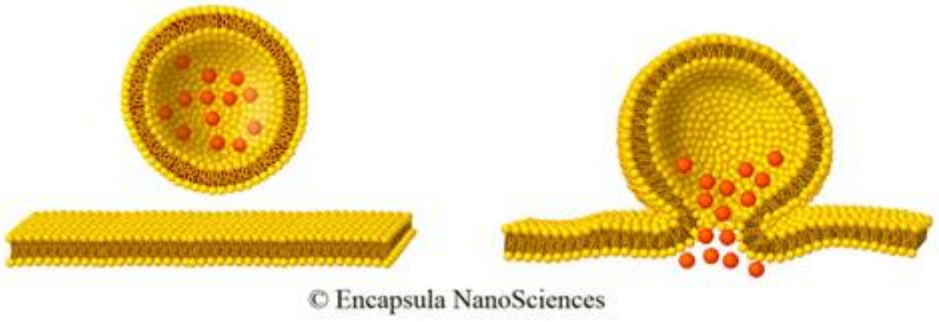

Figure 1.8 The schematic illustration of delivery of drug molecules into the cell.

CHAPTER 2

EXPERIMENTAL PART

2.1 INSTRUMENTS

2.1.1 Fouirer Transform Infrared Spectroscopy (FT-IR)

Fourier transform infrared (FT-IR) spectra were recorded in transmission mode with a Perkin Elmer (FT-IR) infrared spectrometer. FTIR spectra in the range 4000–600 cm^{-1} were recorded in order to investigate the nature of the chemical bonds formed

2.1.2 Nuclear Magnetic Resonance (NMR)

^{1}H NMR spectra were recorded on a Bruker Ultra Shield Plus, Ultra long hold time 400 MHz NMR spectrometer; chemical shifts are expressed in δ ppm with reference to trimethylsilane (TMS). Following solvents were used for the ^{1}H NMR; DMSO-d6, chloroform-d3 ($CDCl_3$), H_2O-d2. These solvents were purchased from Merck.

2.1.3 Melting Point

Melting points were determined on a Mettler FP 80 melting point apparatus.

2.1.4 Scanning Electron Microscopy (SEM)

Field Emission Scanning Electron Microscope (FE-SEM, JEOL 7001 FE) was used in order to investigate the morphology of the samples.

2.1.5 Polarized Optical Microscopy (POM)

Leica DM2500 P polarizing optical microscopy was used in order to investigate the morphology of the samples.

2.1.6 Surface Tension Measurement

The surface tension of aqueous solutions was measured using Wilhelmy Plate method.

2.2 SYNTHESIS

2.2.1 Synthesis of Amino Acid Based Cationic Surfactants

2.2.1.1 Synthesis of C12GluDiamide

BocGluOH was dissolved in 15ml of acetonitrile, together with 2 equivalent of triethylamine and 2 equivalent of BOP. Another 2 equivalent of triethylamine and 2 equivalent of dodecylamine were added simultaneously and the mixture was stirred at room temperature for 1h. The mixture was stirred until obtained solid form. In order to remove HMPT and other impurities the product was dissolved in 50 mL of acetonitrile. After several extractions with acid and basic aqueous solutions, the organic phase was dried over magnesium sulphate, and the solvent removed in vacuo.

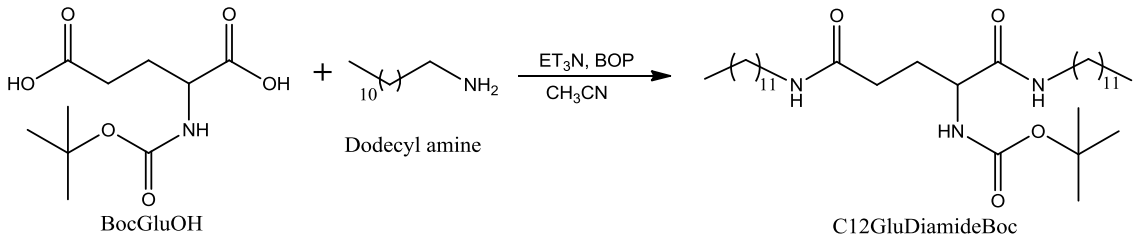

Figure 2.1 Synthesis of C12GluDiamideBoc.

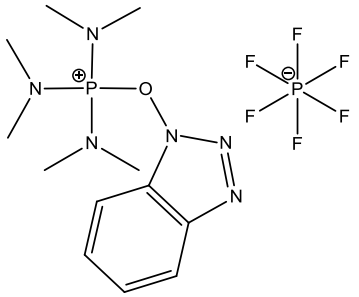

Figure 2.2 BOP coupling reagent.

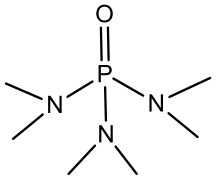

Figure 2.3 The structure of hexamethylphosphoramide.

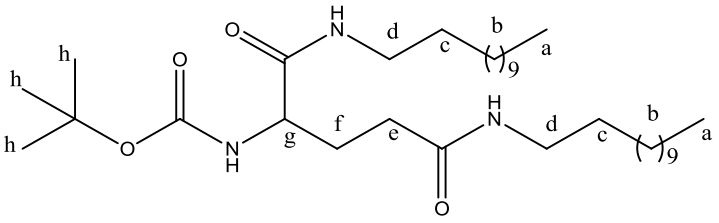

Figure 2.4 The structure of C12GluDiamideBOC.

^{1}H NMR ($CDCl_3$) for C12GluDiamideBOC = **a**, δ=0,89 ppm (t, 6H); **b**, δ=1,26 ppm (s, 36H); **c**, δ=1,51 ppm (p, 4H); **d**, δ=3,25 ppm (m, 4H); **e**, δ=2,3 ppm (m, 2H); **f**, δ=2,05 ppm (m, 2H); **g**, δ=4,08 ppm (q, 1H); **h**, δ=1,45 ppm (s, 9H)

IR ν(CONH) cm^{-1}: 1646 & 1684 **MP (°C):** 96,8 – 99 **Yield:** % 86

After synthesizing C12GluDiamideBOC molecules, the BOC protective group needed to be removed. In order to do this the compound was added in diethyl ether solution, and then allowing HCl gas to pass through the mixture for about 30 minutes. After, the solution was vaporized under vacuum and product was dried.

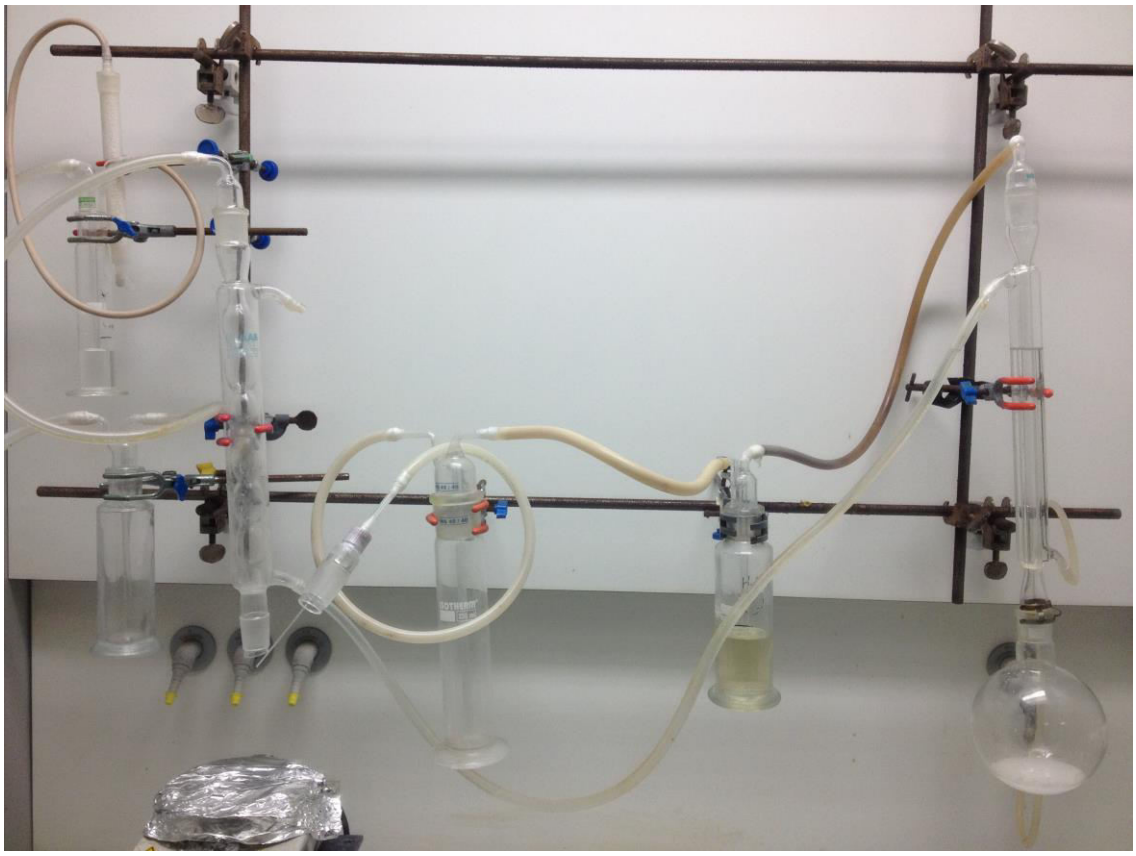

Figure 2.5 HCl gas production set up.

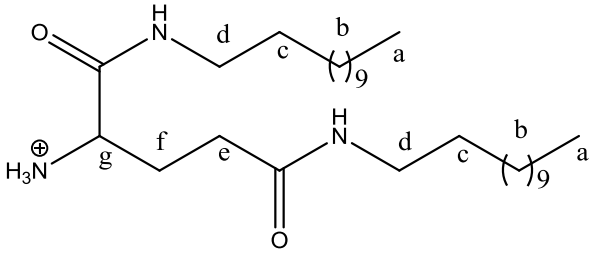

Figure 2.6 The structure of C12GluDiamide.

^{1}H NMR (DMSO) for C12GluDiamide = **a**, δ=0,84 ppm (t, 6H); **b**, δ=1,22 ppm (s, 36H); **c**, δ=1,36 & 1,41 ppm (p, 4H);); **d**, δ=3 & 3,14 ppm (m, 4H); **e**, δ=2,16 ppm (t, 2H); **f**, δ=1,92 ppm (m, 2H); **g**, δ=3,75 ppm (q, 1H).

IR ν(CONH) cm^{-1}: 1649

MP (°C): 150 – 151.1 **Yield:** % 76

2.2.1.2 Synthesis of C12GluDiester

L-glutamic acid (2 gr, 14 mmol) and sulphuric acid (10 drops) was joined in toluene (125 mL). Dodecanol (5,5 gr, 30 mmol) was added to the solution and refluxed with Dean-Stark apparatus for a day at 140°C. The reaction mixture was then evaporated and dissolved in ethyl acetate. The ethyl acetate solution was washed two times with 10% sodium carbonate solution and one times distilled water. After protonated diethyl ether was added to precipitate the product. The product was filtered and washed with diethyl ether. It was further dried in vacuum to obtain a white powder.

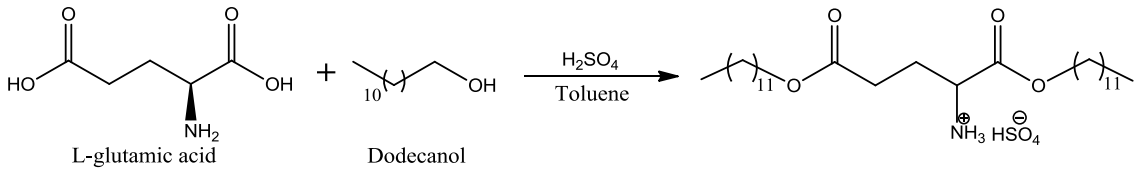

Figure 2.7 Synthesis of C12GluDiester.

Figure 2.8 Dean Stark Apparatus.

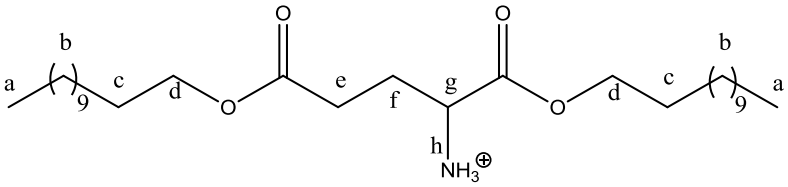

Figure 2.9 The structure of C12GluDiester.

^{1}H NMR($CDCl_3$) for C12GluDiester = **a**, δ=0,84 ppm (t, 6H); **b**, δ=1,23 ppm (s, 38H); **c**, δ= 1,56 ppm (m, 4H); **d**, δ=3,99 ppm (m, 4H); **f**, δ=2,07 ppm (q, 2H); **g**, δ=4,11 ppm (m, 1H); **h**, δ=8,72 ppm (s, 3H)

IR ν(COO$^-$) cm^{-1}: 1733 & 1761

MP (°C): 70.9 – 73.3 **Yield:** % 84

2.2.1.3 Synthesis of C12GluAmidoester

L-Glutamic acid (10 mmol) was joined into water (2 mL) in a round-bottomed flask. Dodecyl amine (10 mmol) in ethanol (6 mL) was added drop by drop under constant stirring at room temperature. The mixture was stirred approximately 15 minutes until a precipitate appears. It is collected on a filter, washed with ethanol and dried in vacuum.

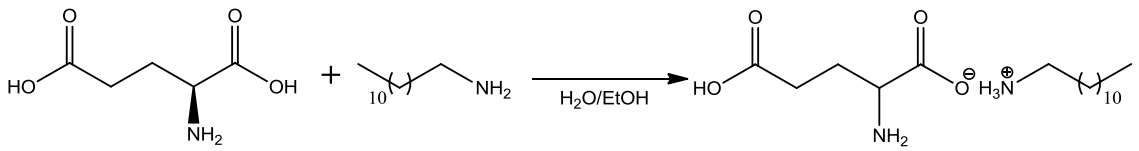

Figure 2.10 Synthesis of Glutamic Acid/Dodecyl Amide Salt.

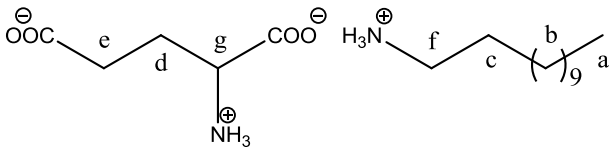

Figure 2.11 The structure of Glutamic Acid/Dodecyl Amide Salt.

^{1}H NMR(D_2O) for C12GluT = **a**, δ=0,84 ppm (t, 3H); **b**, δ=1,25 ppm (m, 18H); **c**, δ= 1,63 ppm (p, 2H); **d**, δ=2,04 ppm (t, 2H); **e**, δ=2,31 ppm (t, 2H); **f**, δ=2,92 ppm (m, 2H); **g**, δ=3,72 ppm (t, 1H)

IR ν(COO$^-$) cm^{-1}: 1656 **MP (°C):** 158 – 159.8 **Yield:** % 96

2 gr. of the product (glutamic acid dodecyl amine salt) was dispersed in 125 mL of xylene in a reactor equipped with a magnetic stirrer and a Dean-Stark separator. After addition of 10 drops of H_2SO_4 the mixture was refluxed until the expected volume of water was obtained (~48 h). The product was diluted with ether and the precipitate filtered off and dried in vacuo. The compound obtained is a white powder.

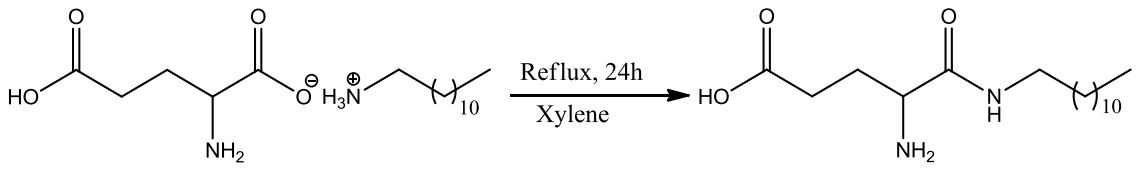

Figure 2.12 Synthesis of C12GluAmide.

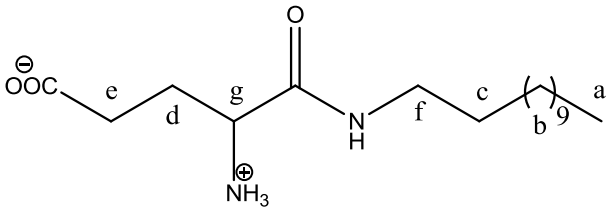

Figure 2.13 The structure of C12GluAmide.

^{1}H NMR($CDCl_3$) for C12GluN = **a**, δ=0,88 ppm (t, 3H); **b**, δ=1,25 ppm (s, 18H); **c**, δ= 1,51 ppm (p, 2H); **d**, δ=2,36 ppm (m, 2H); **e**, δ=2,53 ppm (m, 2H); **f**, δ=3,25 ppm (m, 2H); **g**, δ=4,16 ppm (m, 1H)

IR ν(COO$^-$) cm^{-1}: 1691 **& ν(CONH) cm^{-1}**: 1656

MP (°C): 188 **Yield:** % 89

In order to synthesize C12GluAmidoester, two synthesis methods were tried, but the product could not be obtained. Firstly, C12GluAmide was dispersed in toluene in a reactor equipped with a Dean-Stark separator. After, addition of 1.1 equivalent of H_2SO_4 the mixture is refluxed for 48 h. The solution was vaporized under vacuum. Secondly, C12GluAmide was suspended as slurry in n-dodecanol. Thionyl chloride, 2 equivalents, was slowly added at room temperature and then heated for 3h. The resulting solution was allowed to cool to room temperature and diethyl ether was added to precipitate the product.

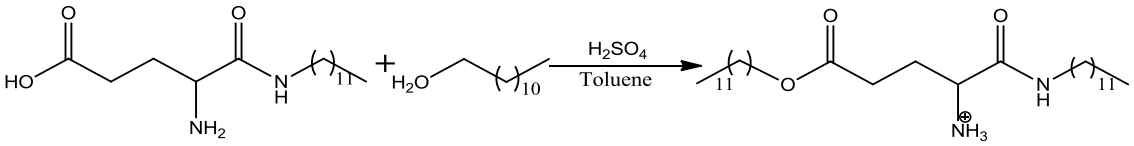

Figure 2.14 Synthesis of C12GluAmidoester in acidic condition.

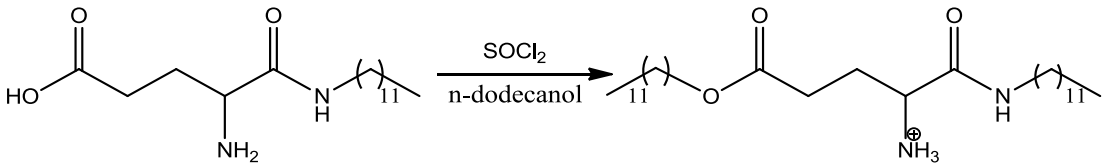

Figure 2.15 Synthesis of C12GluAmidoester with using thionyl chloride.

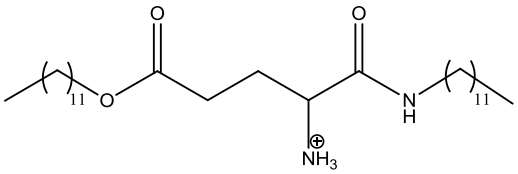

Figure 2.16 The structure of C12GluAmidoester.

2.2.1.4 Synthesis of C12LysineAmidoester

30 mmol NaOH was dissolved in 3 mL water. 30 mmol Lysine monochloride was added to this mixture. Then with a magnetic stirring, this basic mixture was added slowly to ethanol and 30 mmol lauric acid solution. This mixture was stirred until

obtained solid form. After that, the solution was vaporized under vacuum and put inside the desiccators. The compound obtained (lysine lauric acid salt) is a white powder.

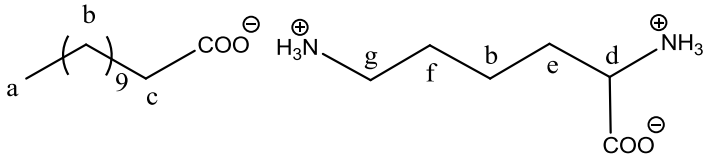

Figure 2.17 The structure of Lysine/Lauric Acid Salt.

^{1}H NMR (D_2O) for C12LysT = **a**, δ=0,8 ppm (t, 3H); **b**, δ=1,23 ppm (s+m,20H); **c**, δ=2,10 ppm (t,2H); **d**, δ=3,62 ppm (t,1H); **e**, δ=1,80 ppm (m, 2H); **f**, δ=1,64 ppm (p, 2H); **g**, δ=2,93 ppm (t, 2H).

IR ν(COO$^-$) cm^{-1}: 1555 **MP** (°C): 162.7 **Yield:** % 87

The product (lysine/lauric acid salt) was dispersed in 125 mL of toluene in a reactor equipped with a magnetic stirrer and a Dean-Stark separator. The mixture was refluxed until the expected volume of water was obtained (~48 h). The solution was vaporized under vacuum and put inside the desiccators. The compound obtained (lysine lauric acid amide) is a cream powder.

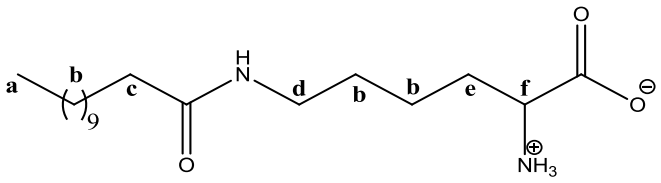

Figure 2.18 The structure of N6-Lauryl-Lysine.

^{1}H NMR (DMSO) for C12LysN = **a**, δ=0,85 ppm (t, 3H); **b**, δ=1,23 ppm (s, 16H); δ=1,39 ppm (p, 2H); δ=1,47 ppm (p, 2H); δ=1,58 ppm (p, 2H) **c**, δ= 2,18 ppm (t, 2H); **d**, δ=3,36 ppm (t, 2H); **e**, δ=1,78 ppm (m, 2H); **f**, δ=3,71 ppm (t, 2H).

IR v(COO$^-$) cm^{-1}: 1696 **& v(CONH) cm^{-1}**: 1651

MP (°C): 172.8 **Yield:** % 76

In order to synthesize C12LysineAmidoester, two synthesis methods were tried, but the product could not be obtained. Firstly, N6-Lauryl-Lysine was dispersed in toluene in a reactor equipped with a Dean-Stark separator. After, addition of 1.1 equivalent of H_2SO_4 the mixture is refluxed for 48 h. The solution was vaporized under vacuum. Secondly, N6-Lauryl-Lysine was suspended as slurry in n-dodecanol. Thionyl chloride, 2 equivalents, was slowly added at room temperature and then heated for 3h. The resulting solution was allowed to cool to room temperature and diethyl ether was added to precipitate the product. After, the product was cooled on ice and the precipitate filtered. Dichloromethane was added to the precipitate and washed with aqueous sodium bicarbonate solution. The organic phase was separated and dried with anhydrous magnesium sulphate, filtered and concentrated under vacuum.

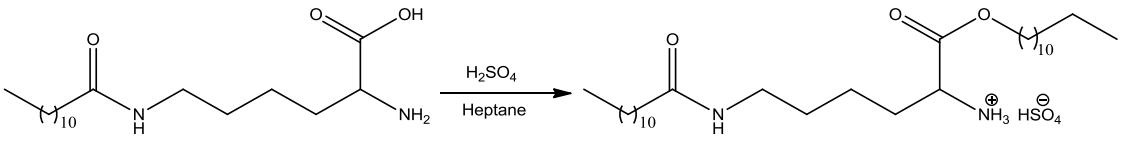

Figure 2.19 Synthesis of C12LysineAmidoester in acidic condition.

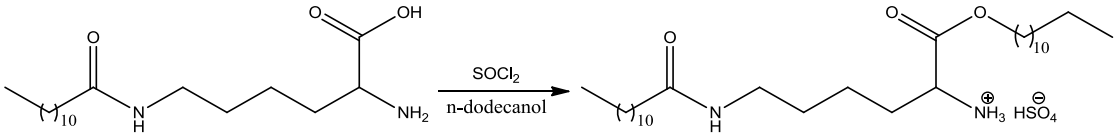

Figure 2.20 Synthesis of C12LysineAmidoester with using thionyl chloride.

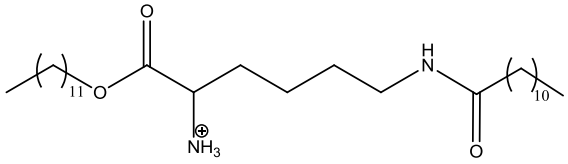

Figure 2.21 The structure of C12LysineAmidoester.

2.2.1.5 Synthesis of C12GluDiamide/Mes-SO_2-Asn-OH Salt

10 mmol NaOH was dissolved in 2 mL water. 10 mmol Mes-SO_2-Asn-OH salt was added to this mixture. Then with a magnetic stirring, this basic mixture was added slowly to ethanol and 10 mmol C12GluDiamide solution. This mixture was stirred until obtained solid form. After that, the solution was filtered under vacuum and put inside the desiccators. The compound obtained is a white powder.

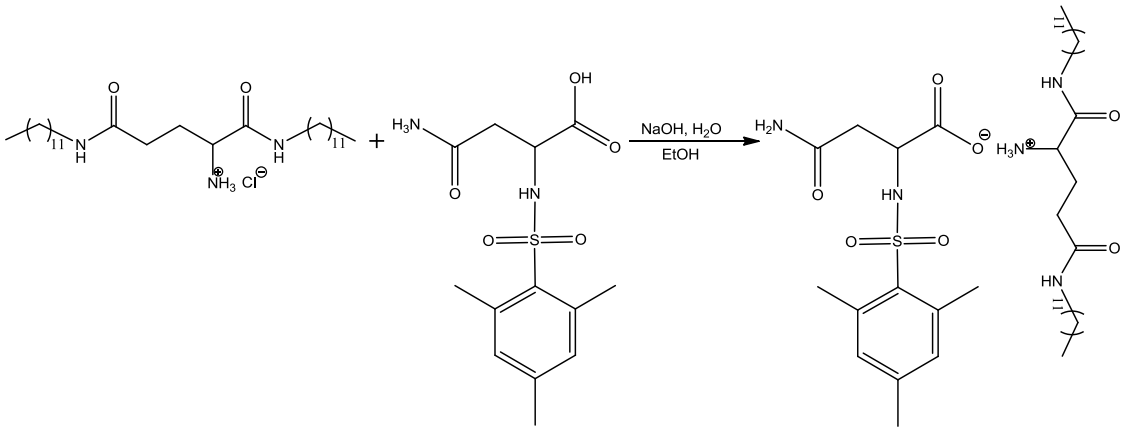

Figure 2.22 Synthesis of C12GluDiamide/Mes-SO_2-Asn-OH Salt.

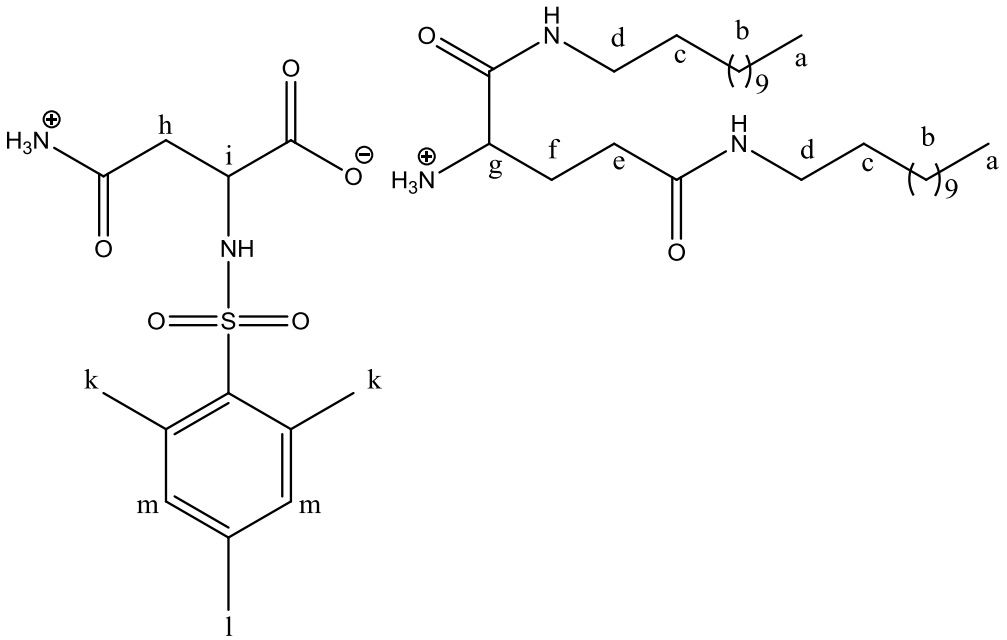

Figure 2.23 The structure of C12GluDiamide/Mes-SO_2-Asn-OH Salt.

^{1}H NMR (CDCl3) for C12GluDiamide/Mes-SO2-Asn-OH Salt = **a**, δ=0,88 ppm (t, 6H); **b**, δ=1,25 ppm (s, 36H); **c**, δ=1,47 ppm (m, 4H); **d**, δ=3,12 & 3,35 ppm (m, 4H); **e**, δ=2,40 ppm (t, 2H); **f**, δ=2,09 ppm (m, 2H); **g**, δ=3,89 ppm (m, 1H); **h**, δ=2,65 ppm (m, 2H); **i**, δ=3,71 ppm (m, 1H); **k**, δ=2,61 ppm (s, 4H); **l**, δ=2,28 ppm (s, 2H); **m**, δ=6,92 ppm (s, 2H).

IR ν(COO$^-$) cm^{-1}: 1651

MP (°C): 121 -123.5 **Yield:** % 96

2.2.1.6 Synthesis of C12GluDiester/Mes-SO$_2$-Asn-OH Salt

In order to make a salt form of C12GluDiester and Mes-SO$_2$-Asn-OH, the following steps were performed, but the salt form of C12GluDiester and Mes-SO$_2$-Asn-OH could not be obtained.

1) Mes-SO$_2$-Asn-OH in water and C12GluDiester in ethanol were mixed.
2) Mes-SO$_2$-Asn-OH and C12GluDiester in ethanol were mixed.
3) Mes-SO$_2$-Asn-OH and 1 eq. NaOH in water were mixed, and then C12GluDiester in ethanol was added.

Because we were unable to obtain the desired product, we decided to carry out different salt formation with C12GluDiester to understand if the amphiphilic molecule makes salt with a carboxyl of another molecule. For this reason, we made salt formation trials with Boc-b-Alanine and salicylic acid, but these experiments also failed.

CHAPTER 3

RESULTS AND DISCUSSION

3.1 AMINO ACID BASED CATIONIC SURFACTANTS

3.1.1 C12GluDiamideBOC

3.1.1.1 FT-IR Analysis

Figure 3.1 shows FT-IR result of the C12GluDiamideBOC molecule. There are three amide bonds in the molecule. In amides, the C=O stretching vibration gives rise to an absorption at 1680-1600 cm^{-1} known as the amide bond and it is strong in the infrared. So, the sharp, strong peak in the 1646 cm^{-1} shows us there must be amide bond. The other peak in the 1684 cm^{-1} must belong to the amide bond of the BOC protecting group, this difference is due to the oxygene connected to the carbonyl carbon of the amide. Trans configuration of the amides can also give peak at 1570-1510 cm^{-1}, involving in plane NH bending and C-N stretching. This band is less intense than the amide bond. The bonds at 1558 cm^{-1} and 1527 cm^{-1} must be because of trans amide bond. And the bond at 3091 cm^{-1} can be overtone of the amide bond. As in amines, the NH stretching vibration gives rise at 3100-3450 cm^{-1} and we can see this stretching at 3308 cm^{-1}.

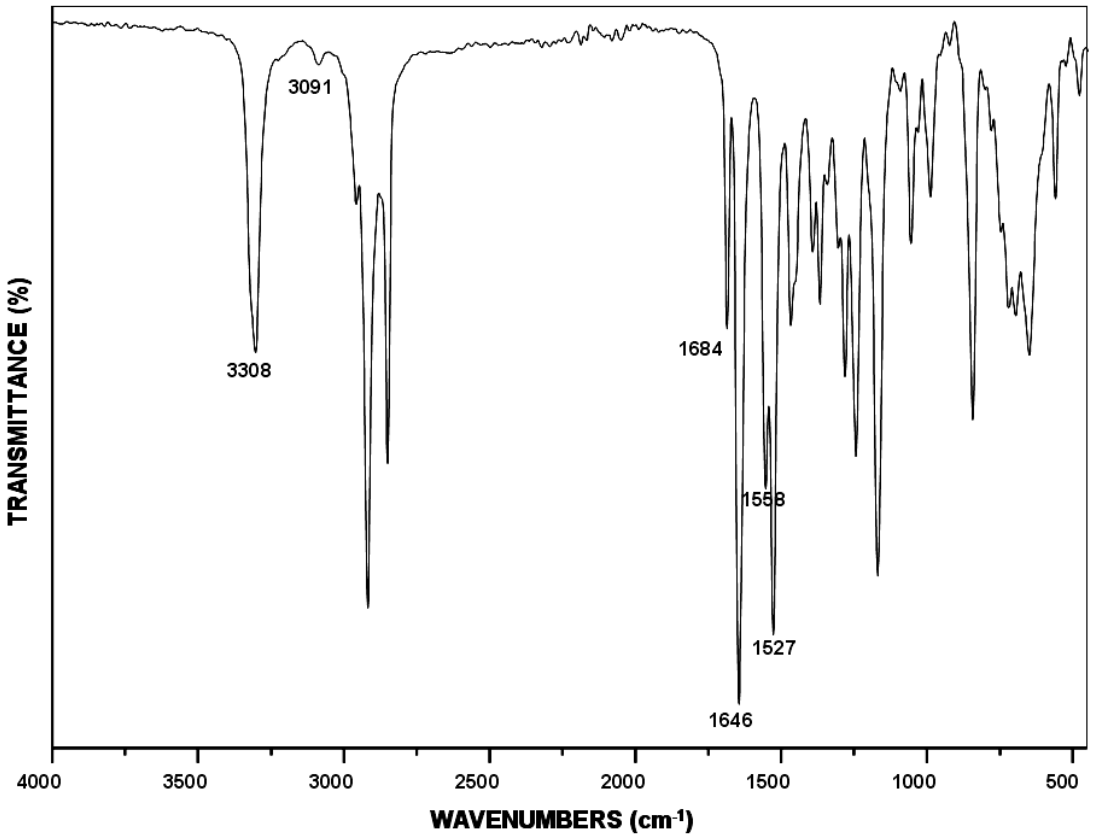

Figure 3.1 ATR spectrum of the C12DiamideBOC molecule.

3.1.1.2 NMR Analysis

The ^{1}H NMR of the C12GluDiamideBOC is on Figure 3.2. We can see the peaks belong to the hydrocarbon chain and glutamic acids' protons around 1 ppm and 2 ppm, respectively. There is also a singlet at 1.45 ppm which belongs to the three metyl group of the BOC protecting group. The most important peak in this NMR spectrum is observed at 3.25 ppm as multiplet. This peak shows the presence of an amide bond in the molecule, because hydrogen in the amide groups has a chemical shift around 3 ppm, generally. Another evidence of the amide bond is the peaks around 6 ppm, there are three peaks which belong to the three amide protons. There is one more singlet around 1.6 ppm, this peak may be occured by the solvent, acetontryl.

Figure 3.2 ^{1}H NMR spectrum of the C12GluDiamideBOC molecule.

3.1.2 C12GluDiamide

3.1.2.1 FT-IR Analysis

Figure 3.3 shows FT-IR result of the C12GluDiamide molecule. The sharp, strong peak in the 1649 cm^{-1} must belong to the two amide bonds. After deprotection, the bond at the 1684 cm^{-1} belong to the amide of BOC protecting group is removed. The peak at 1560 cm^{-1} can be due to plane amide N-H bending and C-N stretching. And the bond at 3095 cm^{-1} can be overtone of the amide bond. We can see stretching of the N-H bonds at 3336 cm^{-1} and 3287 cm^{-1}.

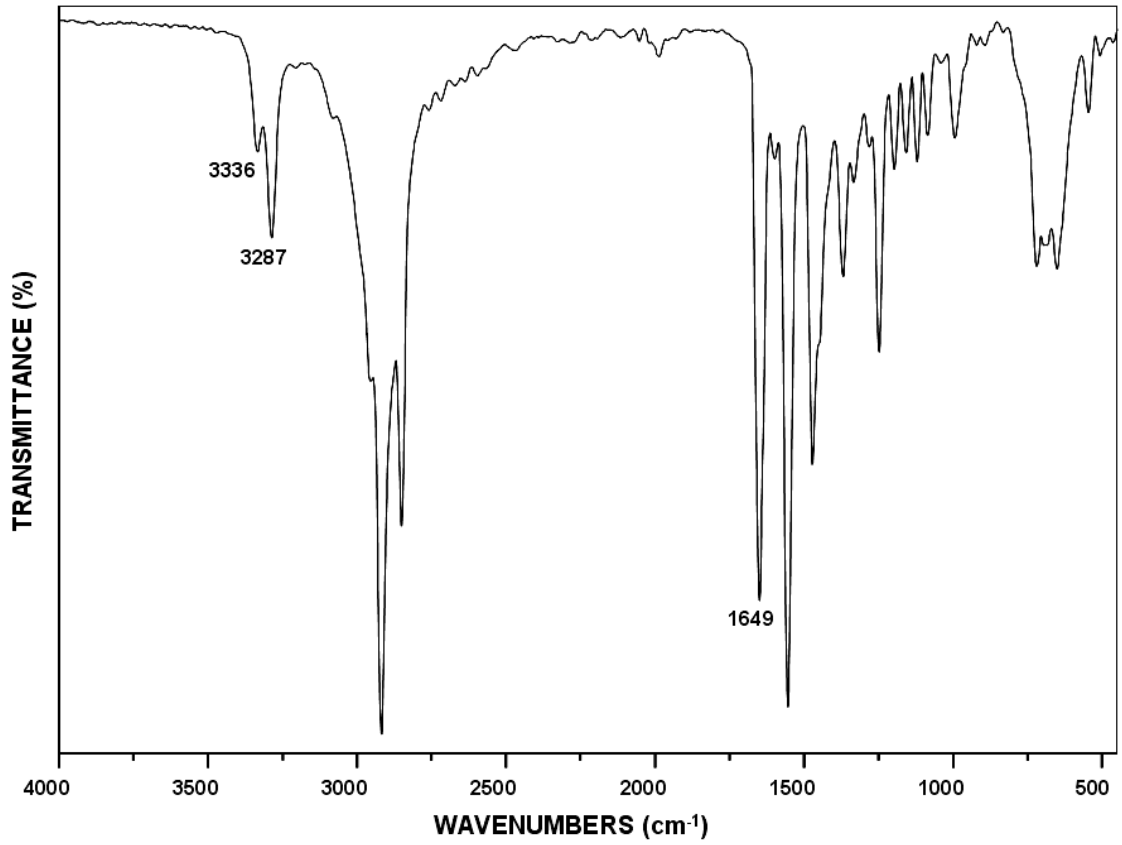

Figure 3.3 ATR spectrum of the C12GluDiamide molecule.

3.1.2.2 NMR Analysis

The ^{1}H NMR of the C12GluDiamide is on the Figure 3.4. After deprotection of the C12GluDiamideBOC, it is need to disappear the proton peaks of BOC protecting group and there is no singlet in 1.45 ppm and around. In the peaks around 8 ppm also shows us, presence of the protons of two amide peaks and the cationic form of the amine.

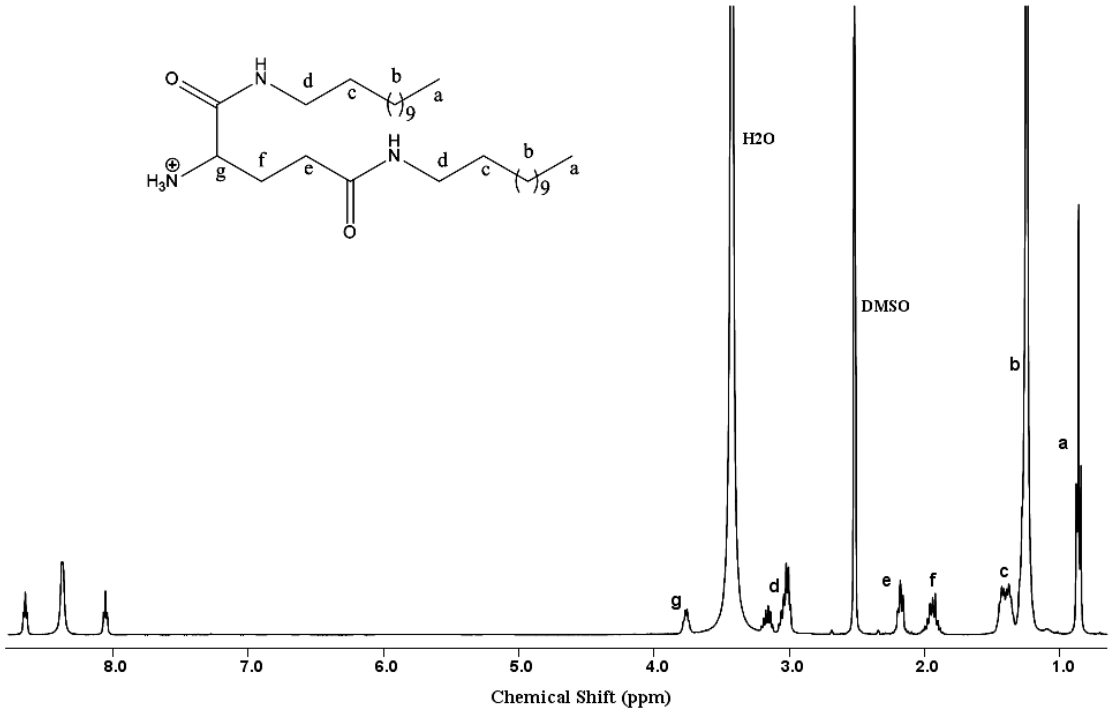

Figure 3.4 ^{1}H NMR spectrum of the C12GluDiamide molecule.

3.1.2.3 POM Analysis

The POM method is particularly useful for the imaging of the microstructures of the large self-assembled aggregates formed in concentrated dispersion. The picture in Figure 3.5 shows us the surface morphology of the C12GluDiamide molecule. There is a wool-like view on the image with a lot of very tiny line. If we compared with the SEM image we can say these very tiny structures can be tubular type aggregation. This is why we saw the gel formation in other POM photograph of the C12GluDiamide. For the gel formation, material should form a network structure with solvent and this was also observed in the solution prepared for the surface tension measurement.

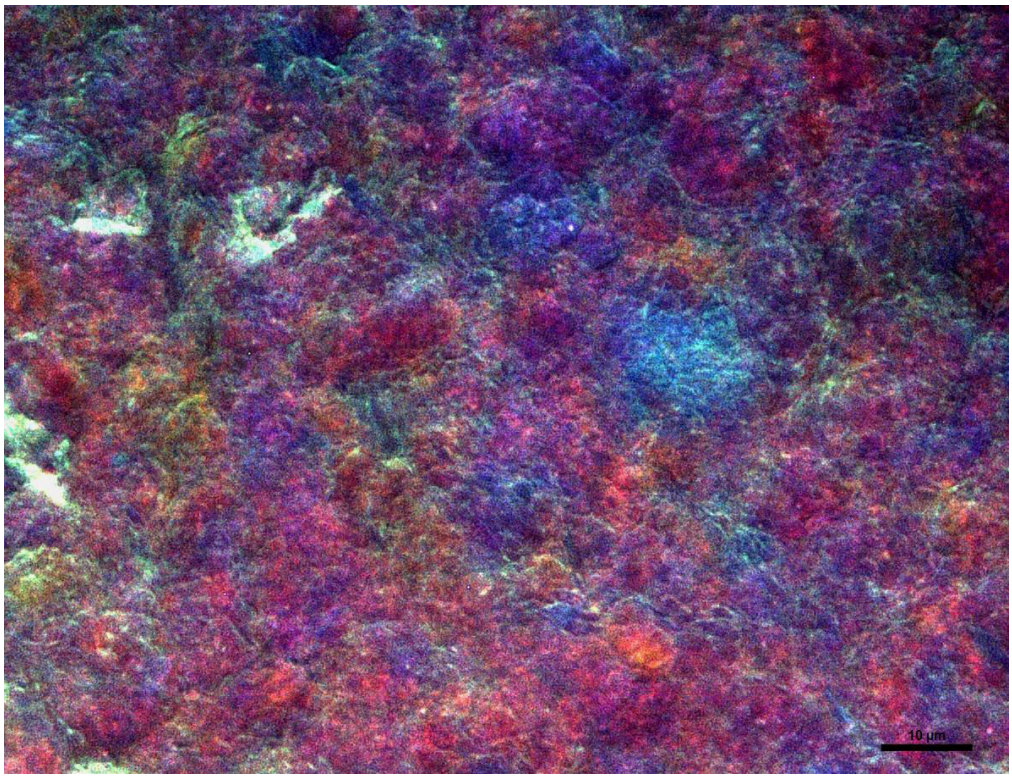

Figure 3.5 POM image of the C12GluDiamide.

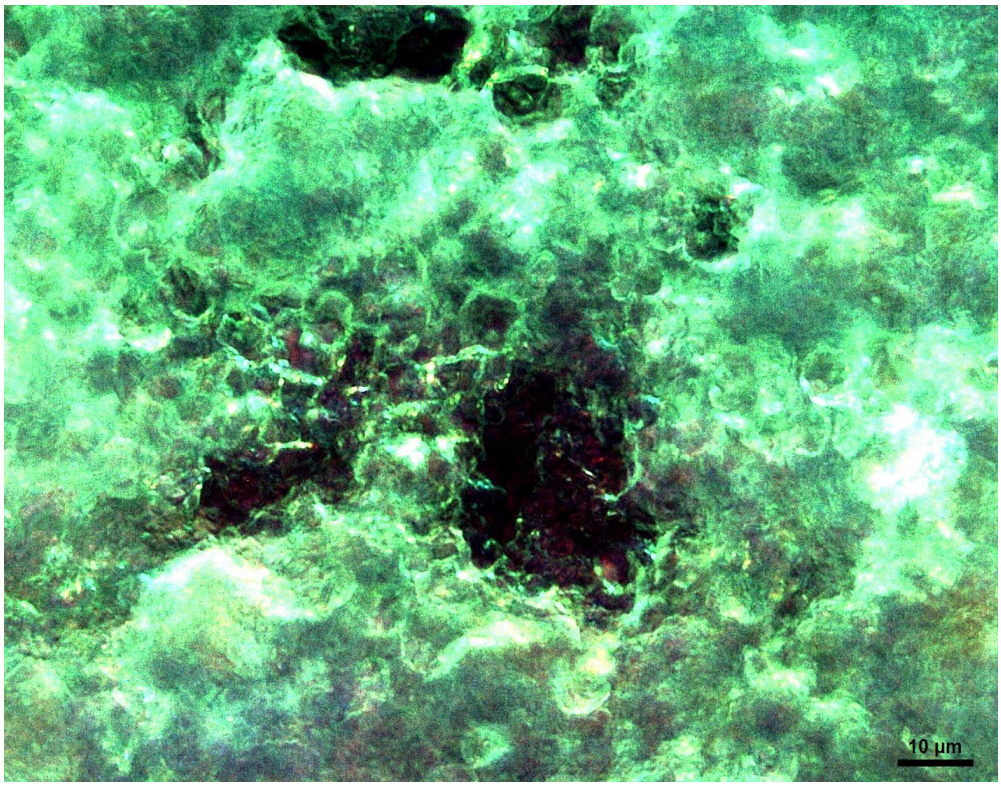

Figure 3.6 Gel formation of the C12GluDiamide with water.

3.1.2.4 SEM Analysis

The SEM photograph of the molecule is shown in Figure 3.7 and Figure 3.8. We can see from the image rod-like micelle type of aggregation can be formed by the C12GluDiamide amphiphilic molecule. The sizes of the tubules are about 0.7μm in diameter. The second SEM photograph also indicates the tubules are in rigid form, while the tubules are flexible with the solvent effect in the POM images.

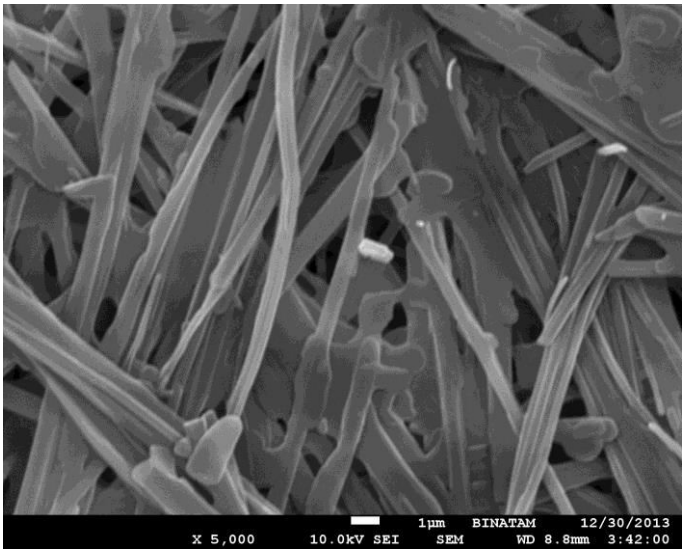

Figure 3.7 SEM image of the C12GluDiamide.

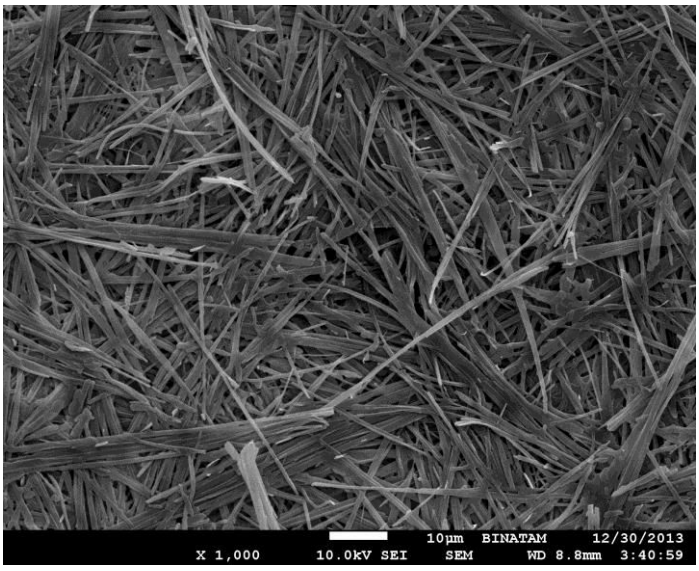

Figure 3.8 SEM image of the C12GluDiamide.

3.1.2.5 The Structure of Optimized C12GluDiamide

The structure of the optimized C12GluDiamide molecule is in the Figure 3.9. The optimization was performed on account of the solvent (water) affect. The maximum effective lengths of the surfactants were calculated from the optimized geometry of the molecule using quantum mechanical force field. The calculated packing parameter of C12GluDiamide is 1.3. According to this result, aggregation type can be reversed micelle, hexagonal etc. If we consider the POM and SEM images of the molecule, we can say that the theoretical and experimental results are compatible. We can see from the experimental results, the amphiphilic molecule has tubular type aggregation. These supramolecular structures seem to be general to a number of surfactants with large headgroups that can form intermolecular hydrogen bonding [31]. Here, molecular packing parameters play an important role, and depending on the headgroup nature and on hydrocarbon chain length. The tubules are firstly fairly rigid self-assemblies, the individual surfactant molecules probably assemble helicoidally and the tubules are hollow.

When compared to physicochemical properties of the two amphiphilic molecules (C12GluDiamide and C12GluDiester) according to their bond type, we can see the difference of the rigid amide bond and flexible ester bond. Both experimental and theoretical results of the C12GluDiamide prove to us this difference. Because of the amide bond, hydrocarbon chains are unable to close each other therefore the distance of two hydrocarbon chains is greater than that with two ester bonds. That is why the packing parameter result of C12GluDiamide is 1.3, while the result of C12GluDiester is 0.87.

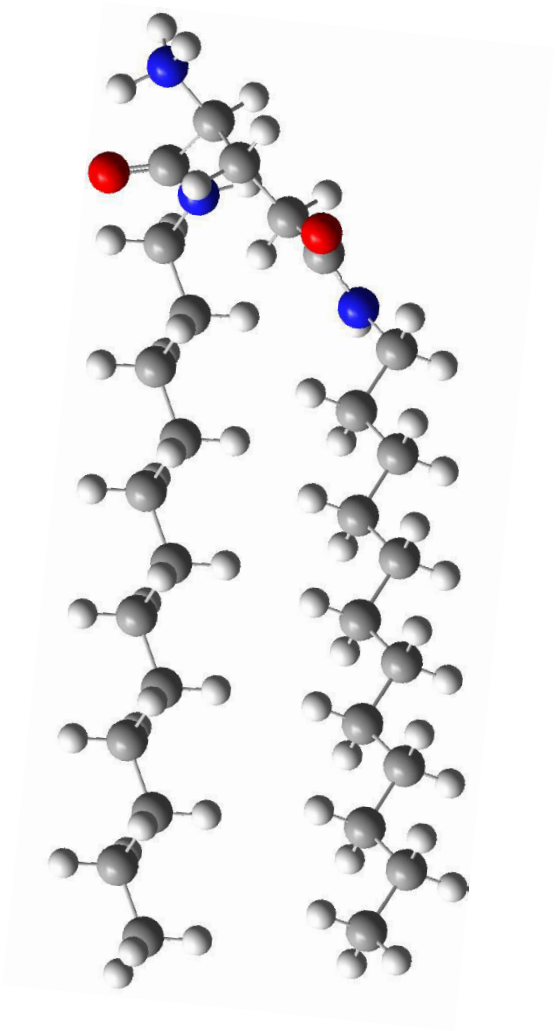

Figure 3.9 Optimized structure of C12GluDiamide.

3.1.2.6 Surface Tension of C12GluDiamide

Surface tension measurements are used to study the various surface phenomena of surfactant systems. In order to detect the critical aggregation concentration, we used the wilhelmy method, C12GluDiamide is 0,0008M.

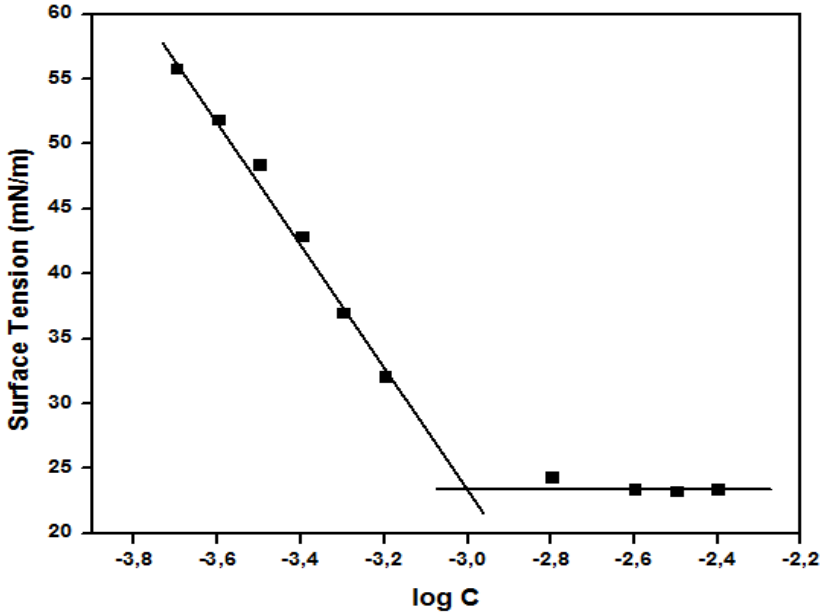

Figure 3.10 Surface tension vs. log concentration curves for the C12GluDiamide.

Table 3.1 The surface tension values of C12GluDiamide molecule.

	CAC ($Mol.L^{-1}$)	$\gamma_{minimum}$ ($mN.m^{-1}$)	Γ ($mole.cm^{-2}$)	σ(wilhemy) ($Å^2$/molécule)	σ(theoretical) ($Å^2$/molécule)
C12GluDiamide	$9,7\ 10^{-4}$	23	$1,52.10^{-10}$	109	29

3.1.3 C12GluDiester

3.1.3.1 FT-IR Analysis

In esters, the C=O stretching vibration gives rise to an absorption band at 1740 cm^{-1} which is very strong and we can see in the Figure 3.11 a strong peak at 1740 cm^{-1}. Another important point for the esters is the C-O stretching. This bond gives the strong peak at 1300-1000 cm^{-1} and we have two strong peaks at 1234 cm^{-1} and 1176 cm^{-1} indicating C-O bonds of the molecule.

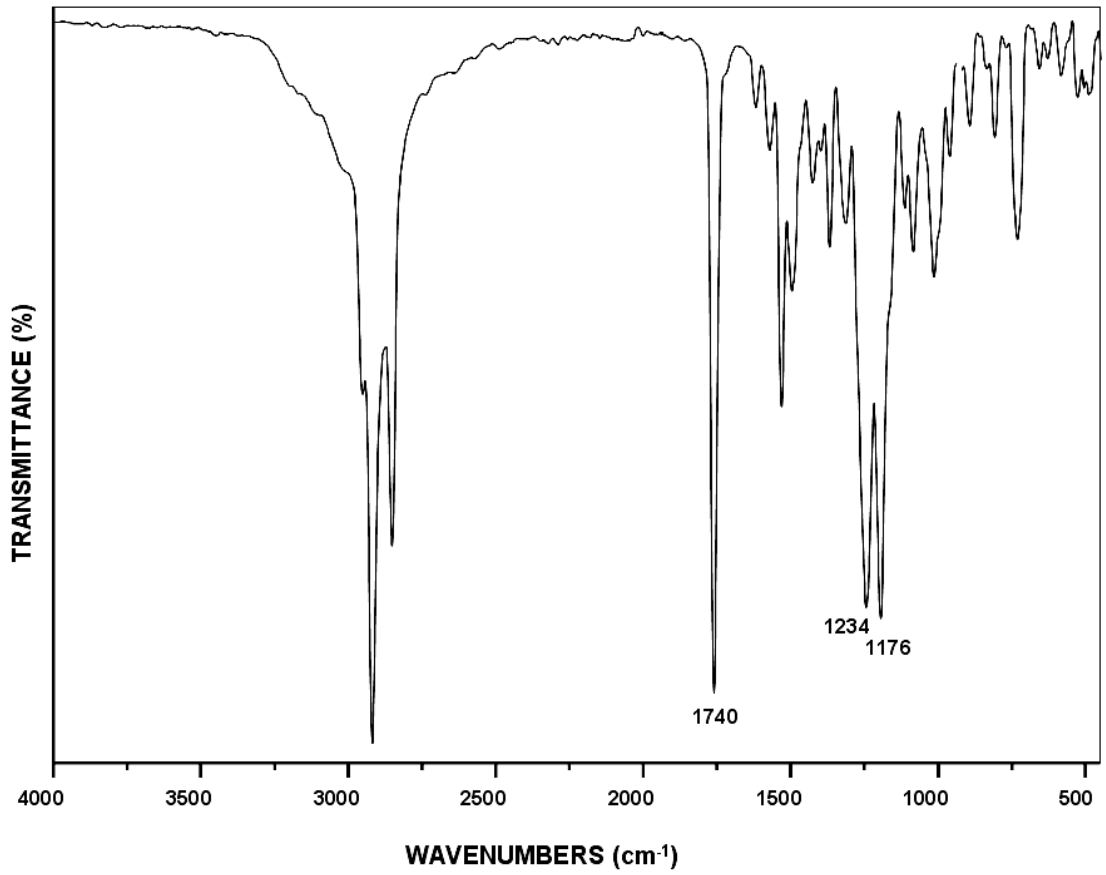

Figure 3.11 ATR spectrum of the C12GluDiester molecule.

3.1.3.2 NMR Analysis

The ^{1}H NMR of the C12GluDiester is very simple. We can see the protons of hydrocarbon chain and amino acid at around 1-2 ppm. The protons of the dodecanol connected to the oxygen atom show the deshielding effects of the electronegative oxygen atom. In general, the chemical shift of protons on the carbon atom connected to the ester group is around 4 ppm. So, we can say there are two ester bonds in the molecule.

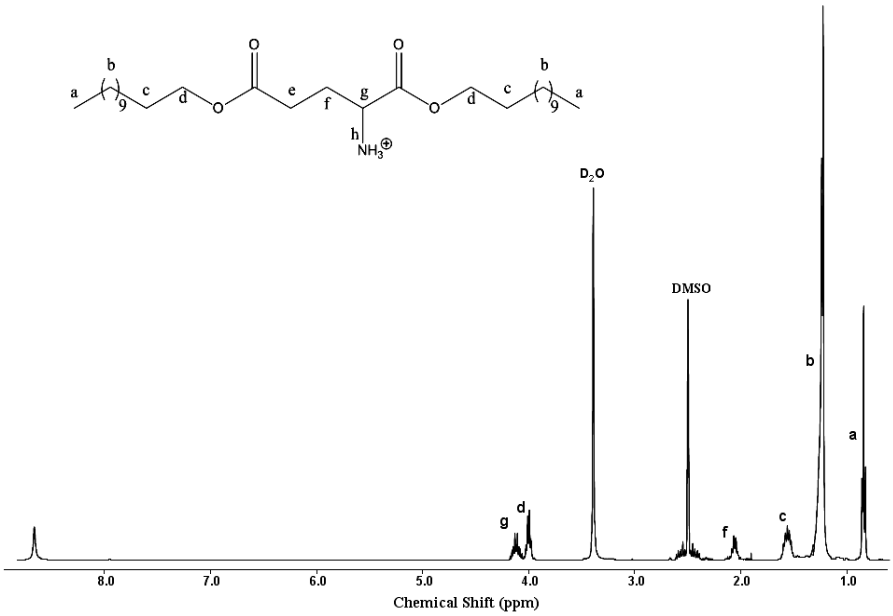

Figure 3.12 ^{1}H NMR spectrum of the C12GluDiester molecule.

3.1.3.3 POM Analysis

To determine the aggregation morphologies of the C12GluDiester with water, the POM was performed. A lot of circular structures of different size can be seen on the image. The structure of the molecule can be flexible planar geometry which is compatible with the SEM image.

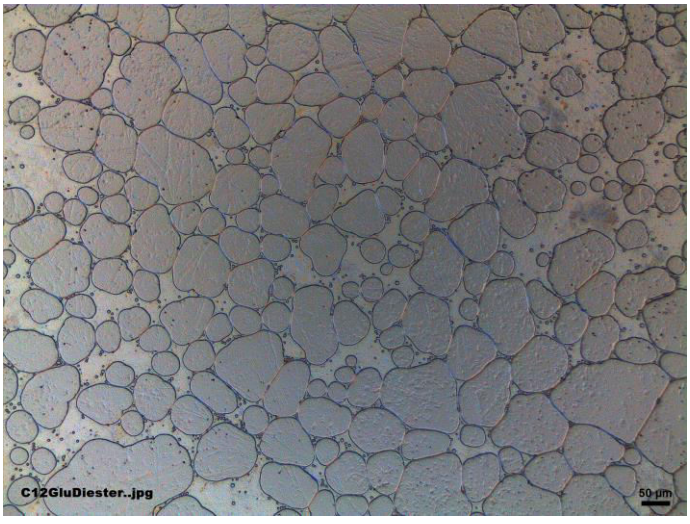

Figure 3.13 POM image of the C12GluDiester.

3.1.3.4 SEM Analysis

The SEM picture of the molecule can be seen on the Figure 3.14. As a result of the interaction of the molecules, the C12GluDiester amphiphiles have flexible planar geometry with ~0.3 μm tickness.

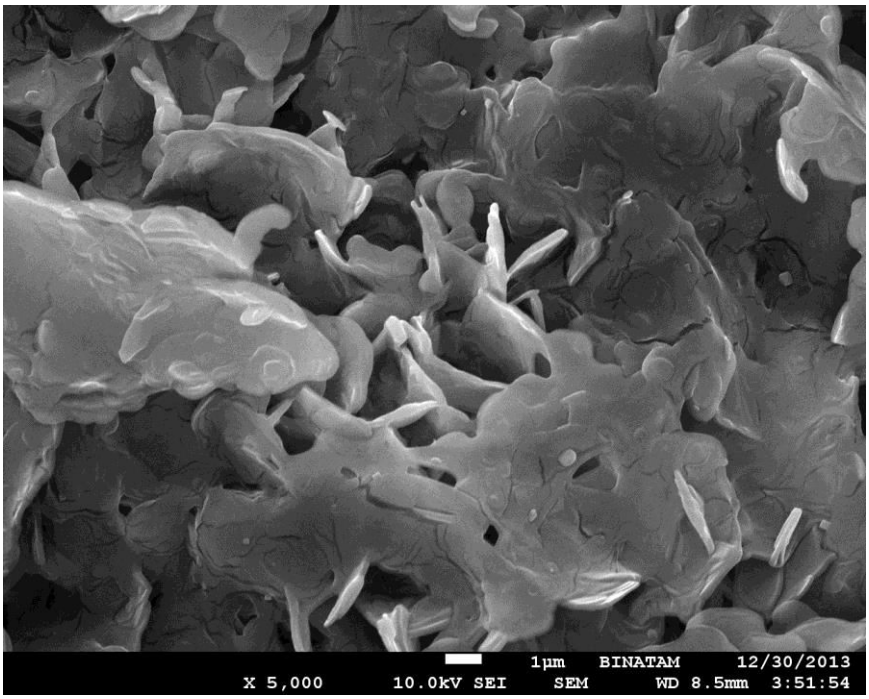

Figure 3.14 SEM image of the C12GluDiester.

3.1.3.5 The Structure Of Optimized C12GluDiester

The structure of the optimized C12GluDiester molecule is on the Figure 3.15. Calculated packing parameter of C12GluDiester is 0.87. According to the packing parameter table, we can hope to see the flexible lamellar structure or vesicle type aggregation depens on the result. The SEM and POM images of the amphiphilic molecule also support the result of the calculated packing parameter.

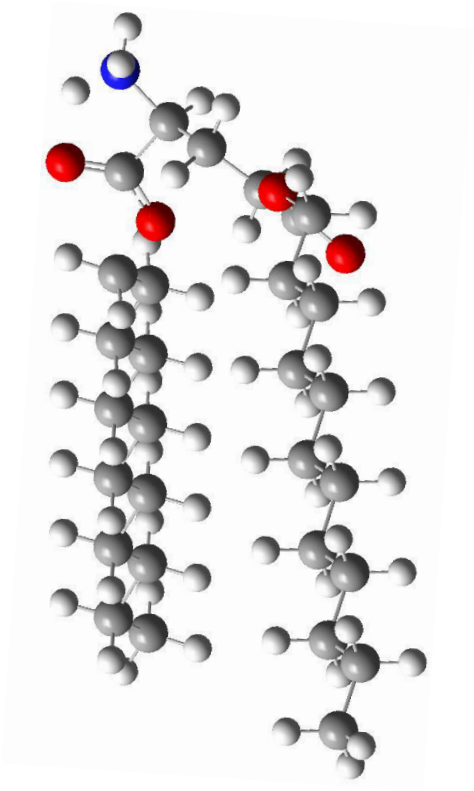

Figure 3.15 Optimized structure of C12GluDiester.

3.1.3.6 Surface Tension of C12GluDiester

Determination of the CAC by tensiometry provides an opportunity to determine the packing of the surfactant at the air-water interface. According to the Wilhelmy method's result, the critical aggregation concentration of the C12GluDiester was found as 0.0025M.

Table 3.2 The surface tension values of C12GluDiester molecule.

	CAC ($Mol.L^{-1}$)	$\gamma_{minimum}$ ($mN.m^{-1}$)	Γ ($mole.cm^{-2}$)	σ(wilhemy) ($Å^2$/molecule)	σ(theoretical) ($Å^2$/molecule)
C12GluDiester	$2,5\ 10^{-3}$	34,6	$1,25.10^{-10}$	133	34

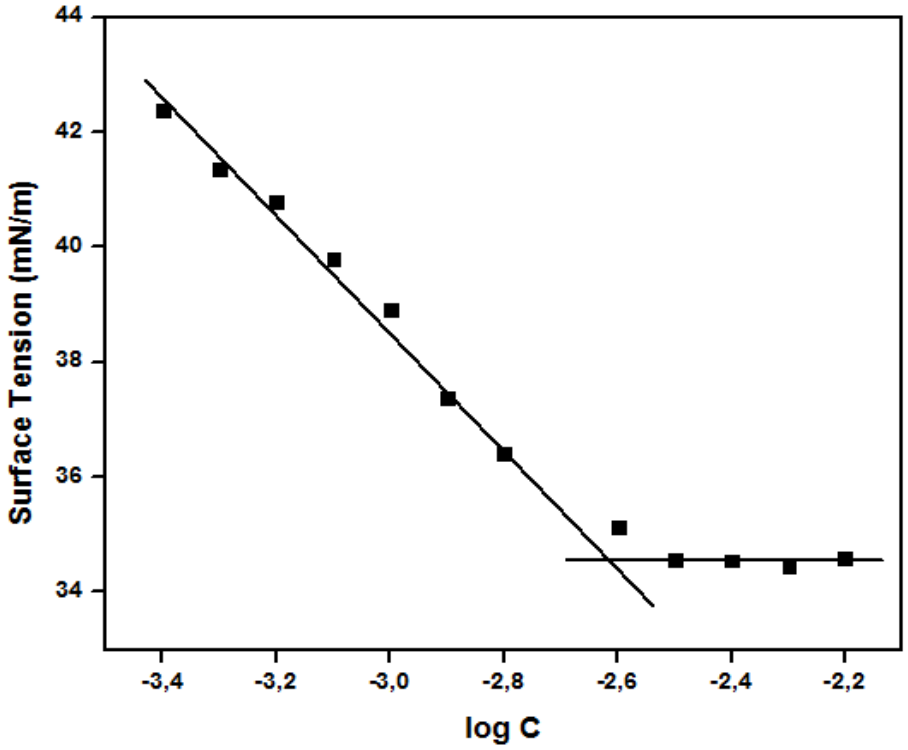

Figure 3.16 Surface tension vs. log concentration curves for the C12GluDiester.

3.1.4 Glutamic Acid/Dodecyl Amine Salt

3.1.4.1 FT-IR Analysis

In carboxylate salts, the two identical C=O bonds give rise; the antisymmetric CO_2 stretching vibration at 1650-1550 cm^{-1} is very strong in the infrared, while corresponding symmetric vibration at 1450-1350 cm^{-1} is weaker in the infrared. The antisymmetric CO_2 stretchs of the glutamic acid can be 1656 cm^{-1} and 1600 cm^{-1}. There is a broad peak at 2000-3500 cm^{-1}, this peak can belong to the carboxylic acid or an attraction can cause these vibrations in between carbonyl group (COO^-) and alpha amino group (NH_3^+).

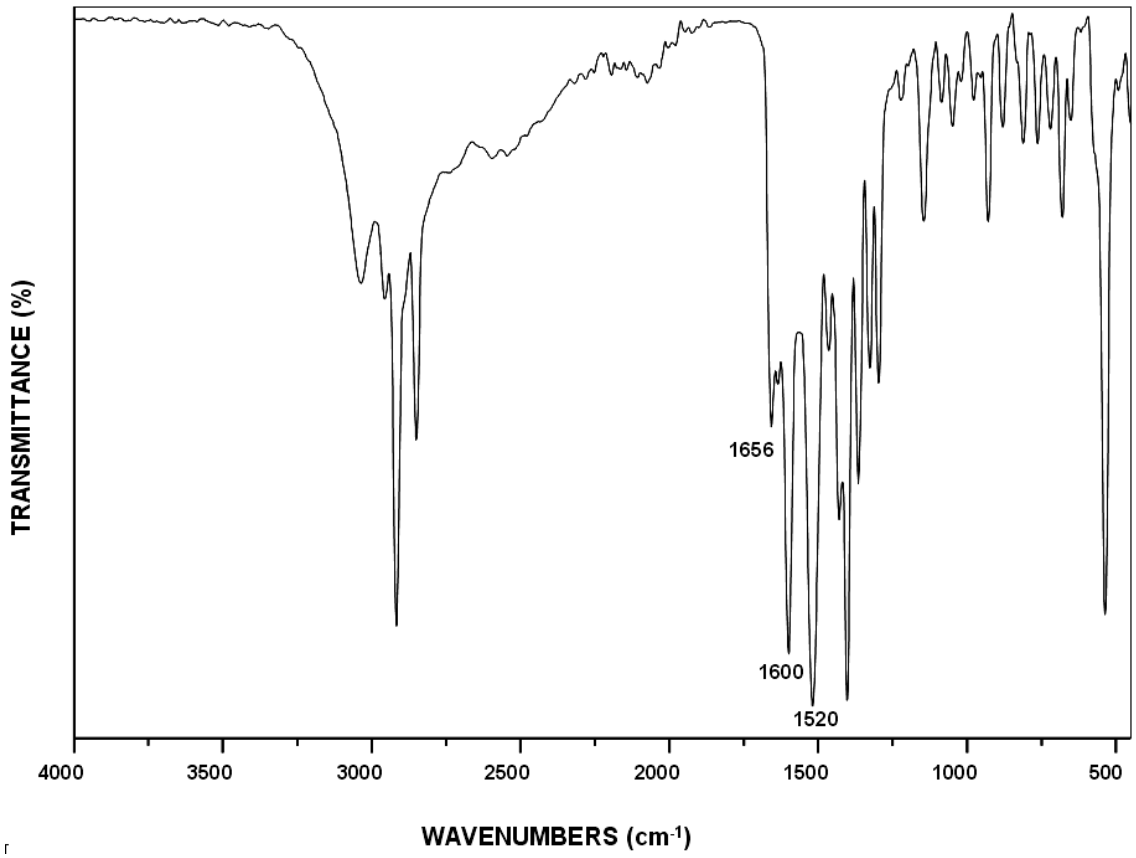

Figure 3.17 ATR spectrum of the Glutamic Acid/Dodecyl Amide Salt molecule.

3.1.4.2 NMR Analysis

The ^{1}H NMR of the Glutamic Acid/Dodecyl Amine Salt is on the Figure 3.18. Actually, there is no peak to understand the formation of the salt, because there is no certain bond formed by the reaction. These two substances connect each other with electrostatic attraction and both of them show same peaks with their individual form in NMR, but integration of the protons let us to know whether the substance is salt and we were clearly seen this in the proton NMR.

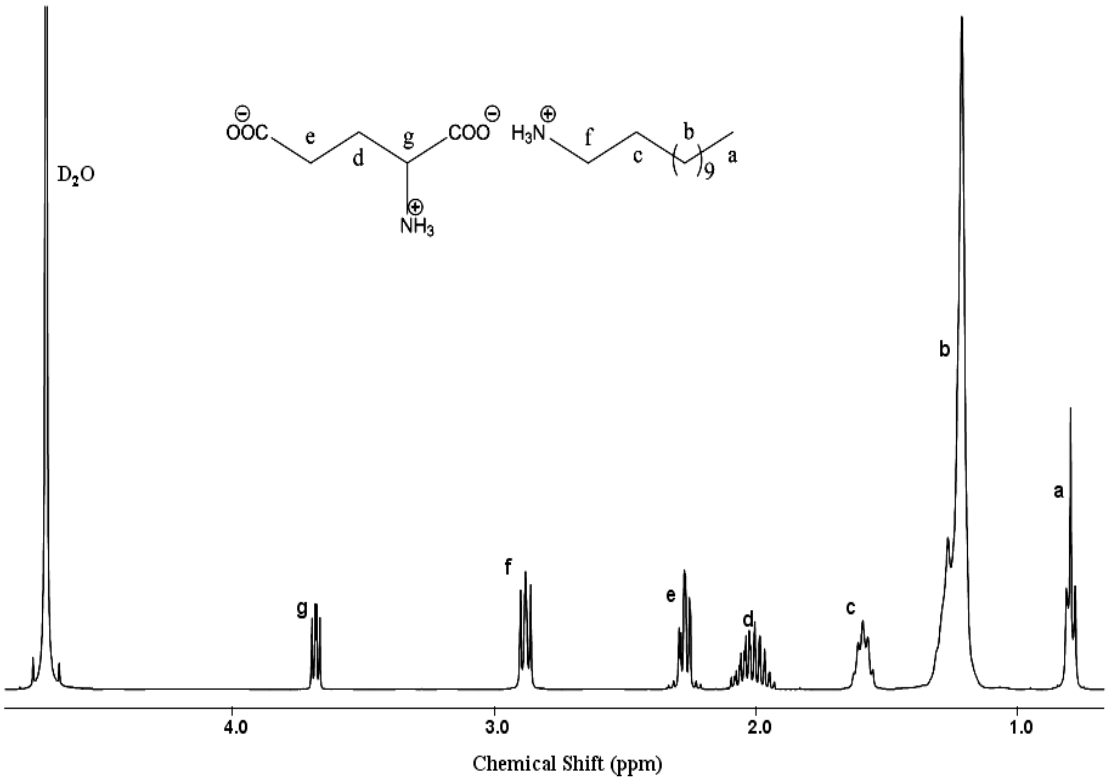

Figure 3.18 ^{1}H NMR spectrum of the Glutamic Acid/Dodecyl Amine Salt molecule.

3.1.5 C12GluAmide

3.1.5.1 FT-IR Analysis

C12GluAmide have both carboxyl and amide forms of the carbonyl. We can see the carbonyl stretching of the amide at 1656 cm^{-1} and it's overtone at 3095 cm^{-1} the peak at 1550 cm^{-1} can be related with the trans configuration of the amide bond. The strong, sharp peak at 1691 cm^{-1} can belong to the carbonyl carbon of the carboxylic acid. Hydrogen stretching of the amine group and amide bond can be seen at 3283 cm^{-1} and 3221 cm^{-1}.

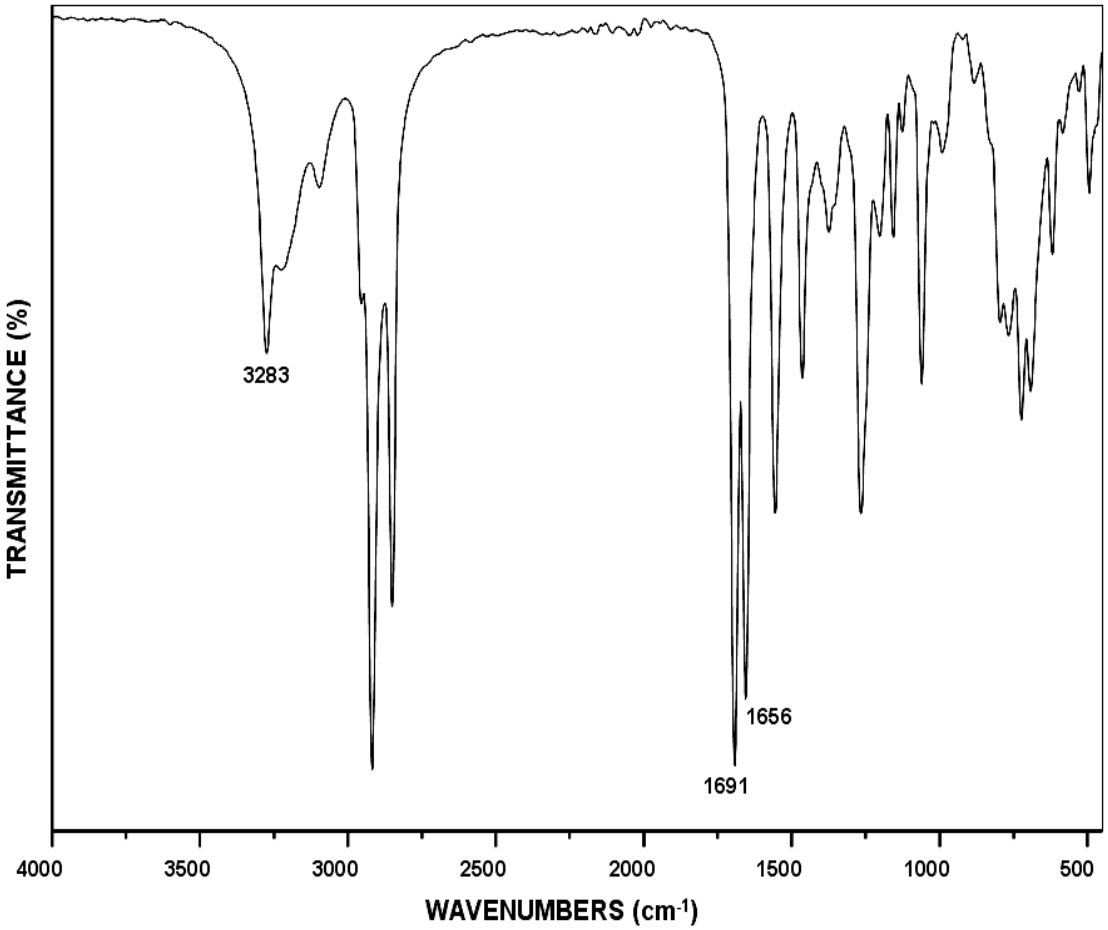

Figure 3.19 ATR spectrum of the C12GluAmide molecule.

3.1.5.2 NMR Analysis

The ^{1}H NMR of the C12GluAmide is on the Figure 3.20. The formation of the amide bond is clearly seen in the proton NMR. The hydrogen protons on the carbon connected to the amide group appears as a quartet at 3.25 ppm. We can also see the hydrogen peaks of the amin and the amide at around 7 ppm.

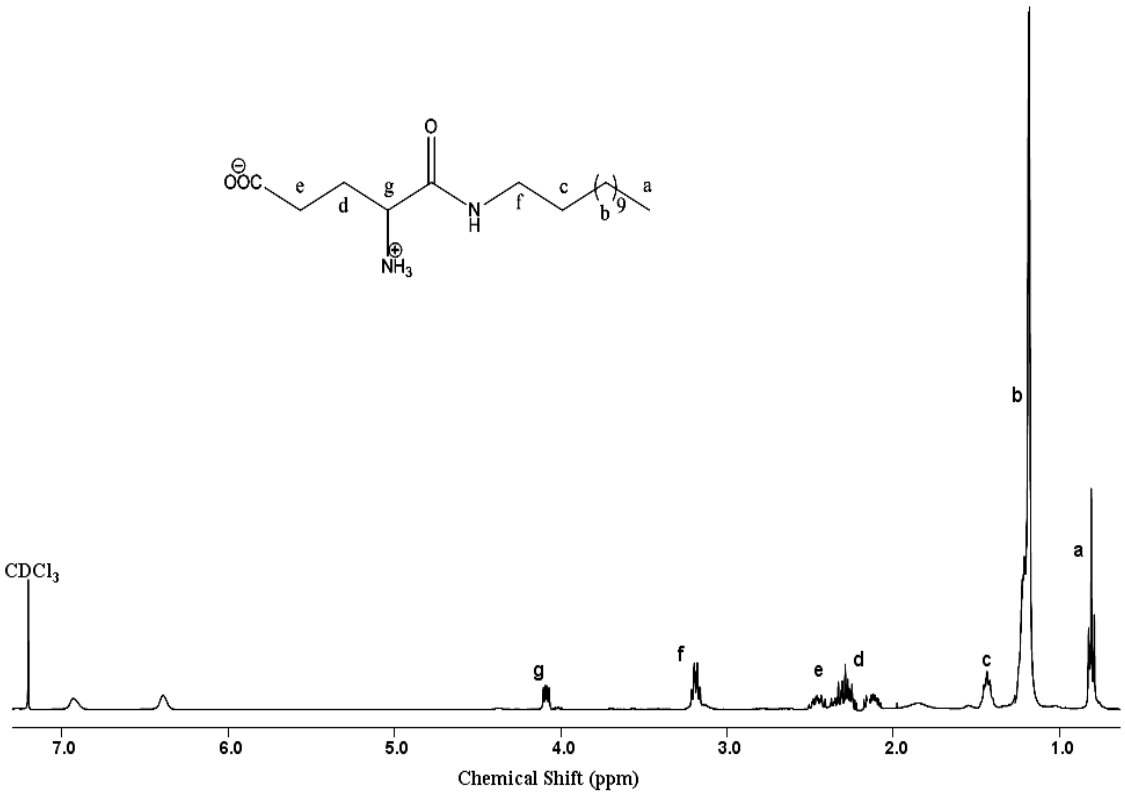

Figure 3.20 ^{1}H NMR spectrum of the C12GluAmide molecule.

3.1.6 Lysine/Lauric Acid Salt

3.1.6.1 FT-IR Analysis

In carboxylate salts, the two identical C=O bonds give rise; the antisymmetric CO_2 stretching vibration at 1650-1550 cm^{-1} is very strong in the infrared. We can see a very strong peak at 1556 cm^{-1} in the Lysine/Lauric Acid Salt's ATR result. There are also two broad peak at 3478 & 3379 cm^{-1} that may belong to the amino groups of the lysine.

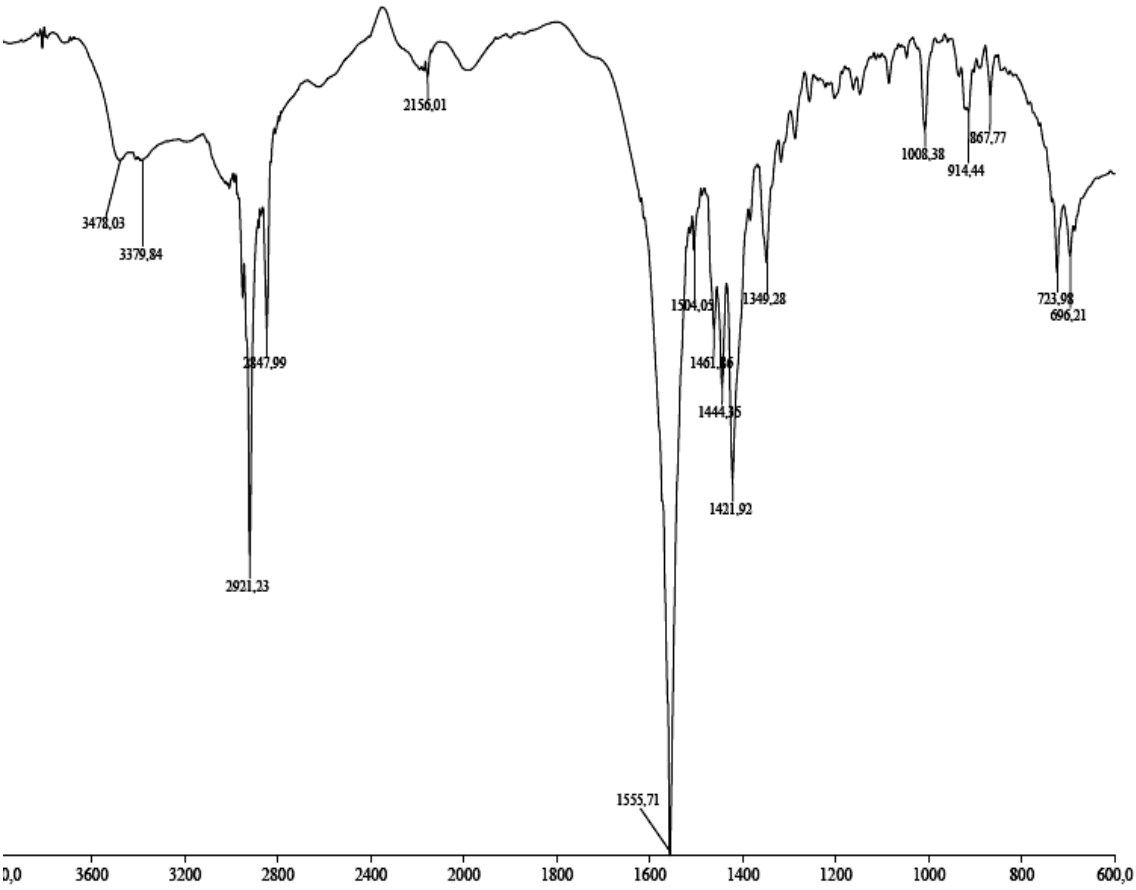

Figure 3.21 ATR spectrum of the Lysine/Lauric Acid Salt.

3.1.6.2 NMR Analysis

^{1}H NMR spectrum of the lysine/lauric acid salt is on the Figure 3.22. We can see clearly all peaks of the molecule in the proton NMR. The CH_3 and CH_2 protons on the dodecanoic acid have chemical shift at 0.8 ppm, 1,23 ppm and 2.10 ppm, respectively. The CH_2 connected to the carboxyl group shifts to downfield because of the electronegativity of the carboxyl group. And the protons of the lysine are at around 2 and 3 ppm depends on their neighbour elements.

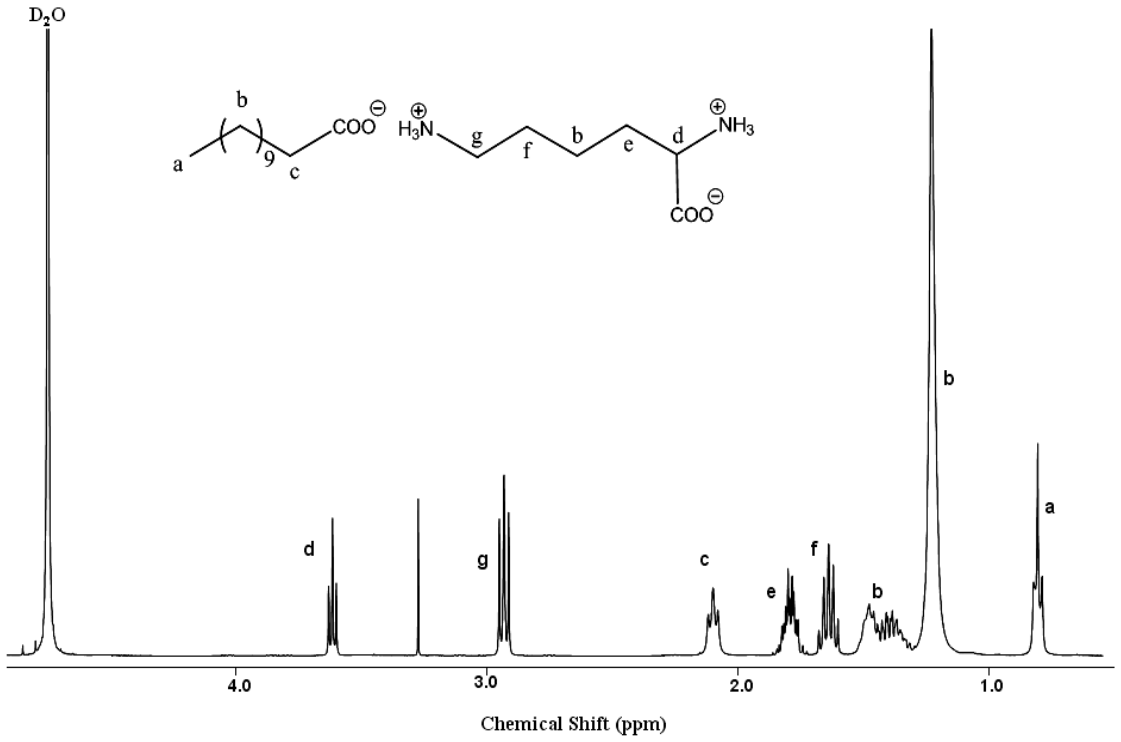

Figure 3.22 ^{1}H NMR spectrum of the lysine/lauric acid salt molecule.

3.1.7 C12LysineAmide

3.1.7.1 FT-IR Analysis

Figure 3.23 shows FT-IR result of the C12LysineAmide molecule. After amidation of the Lysine/Lauric Acid Salt, we expect to see amide bond in the FT-IR result and to remove the peak of the carboxylic acid salt in 1555 cm^{-1}. As can be seen on the ATR result, we have an amide bond at 1651 cm^{-1} and the carboxylic acid vibration of the lysine at 1696 cm^{-1}. The C-O stretching of the carboxylic acid is at 1137 cm^{-1}.

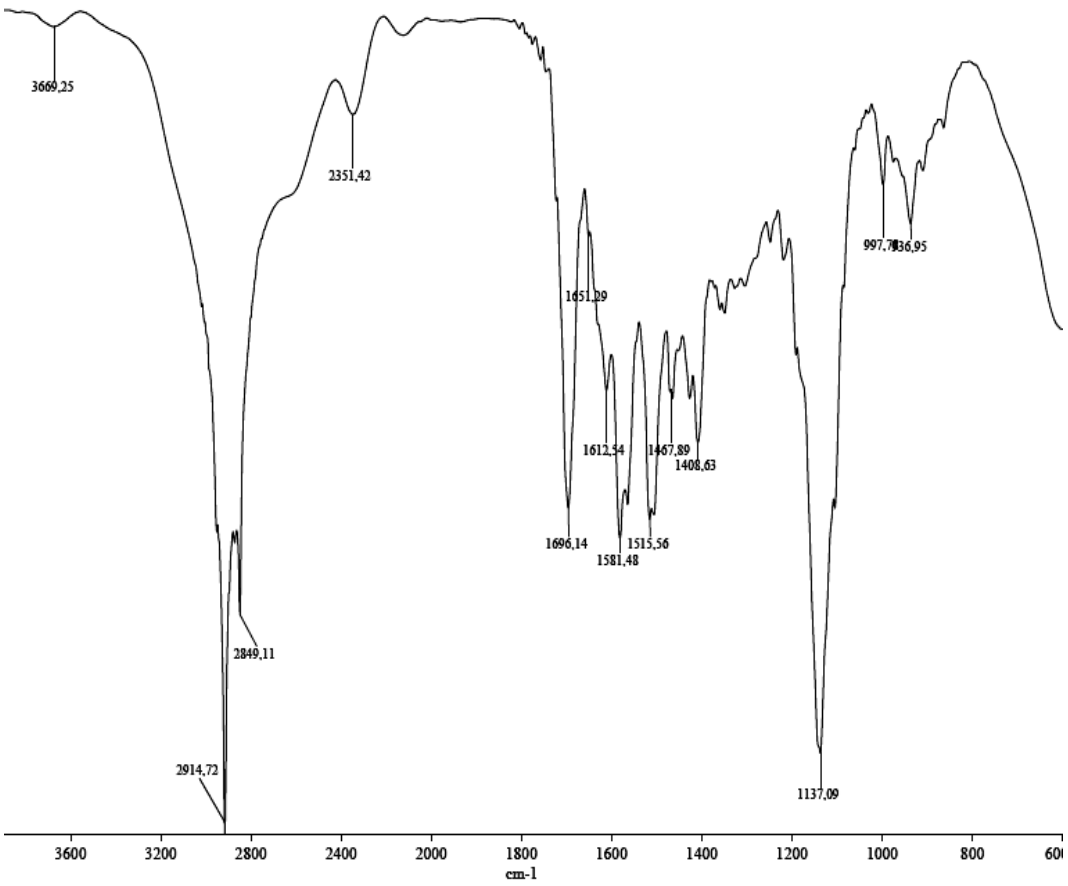

Figure 3.23 ATR spectrum of C12LysineAmide.

3.1.7.2 NMR Analysis

^{1}H NMR spectrum of the C12LysineAmide is shown in Figure 3.24. The most important peak in this spectrum is at 3.36 ppm. This peak proves to us there is an amide in the molecule. The CH_2 connected to the nitrogen shifts to downfield because of the electronegativity of the amide group.

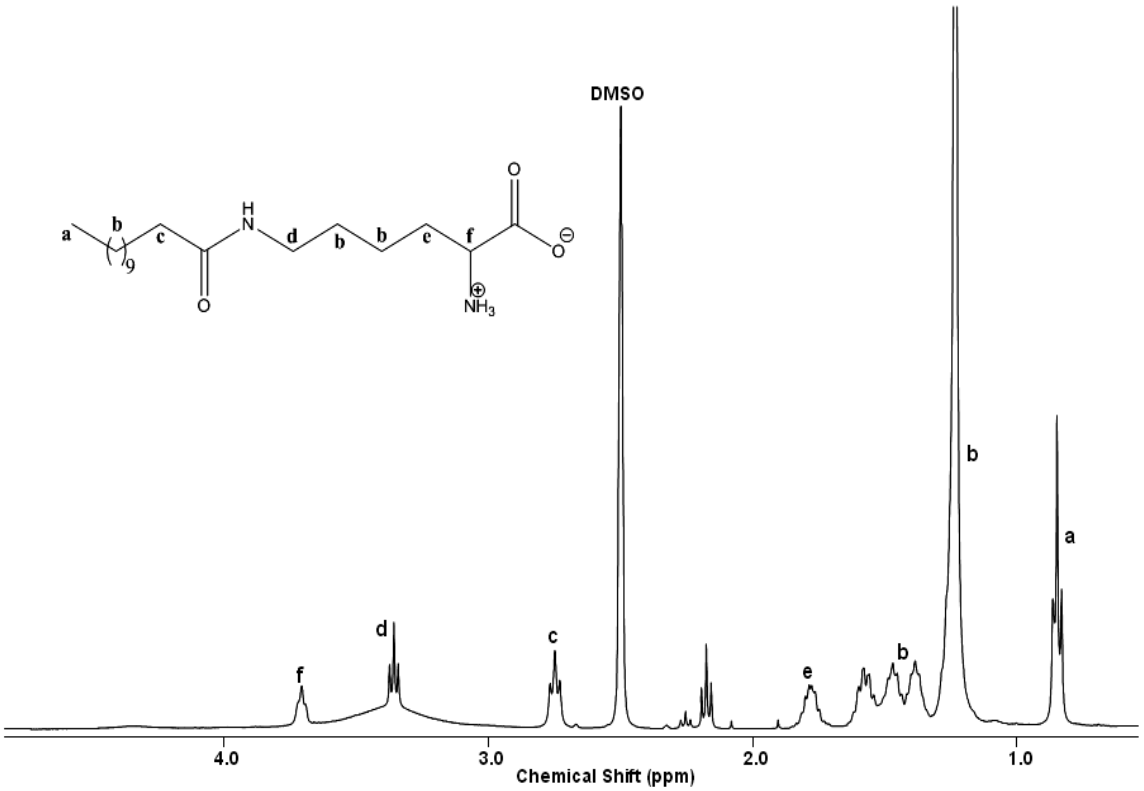

Figure 3.24 ^{1}H NMR spectrum of C12LysineAmide.

3.1.8 C12GluDiamide/Mes-SO_2-Asn-OH Salt

3.1.8.1 FT-IR Analysis

The CO_2 stretching vibration of carboxylic salt is at 1603 cm^{-1} in the infrared. We can see the amide peak of the C12Diamide at 1651 cm^{-1} and amide protons at 3291 cm^{-1}. The aromatic ring's C=C bending can be the strong peak at 1560 cm^{-1} and C=H bending at 687 cm^{-1}. The C=H stretching of the aromatic protons can be seen at 3027 cm^{-1} and the aromatic patterns at around 2000 cm^{-1}. We have three amide and two amine group in the molecule and there are a few peaks on the ATR spectrum which may belong to these hydrogen strecthings.

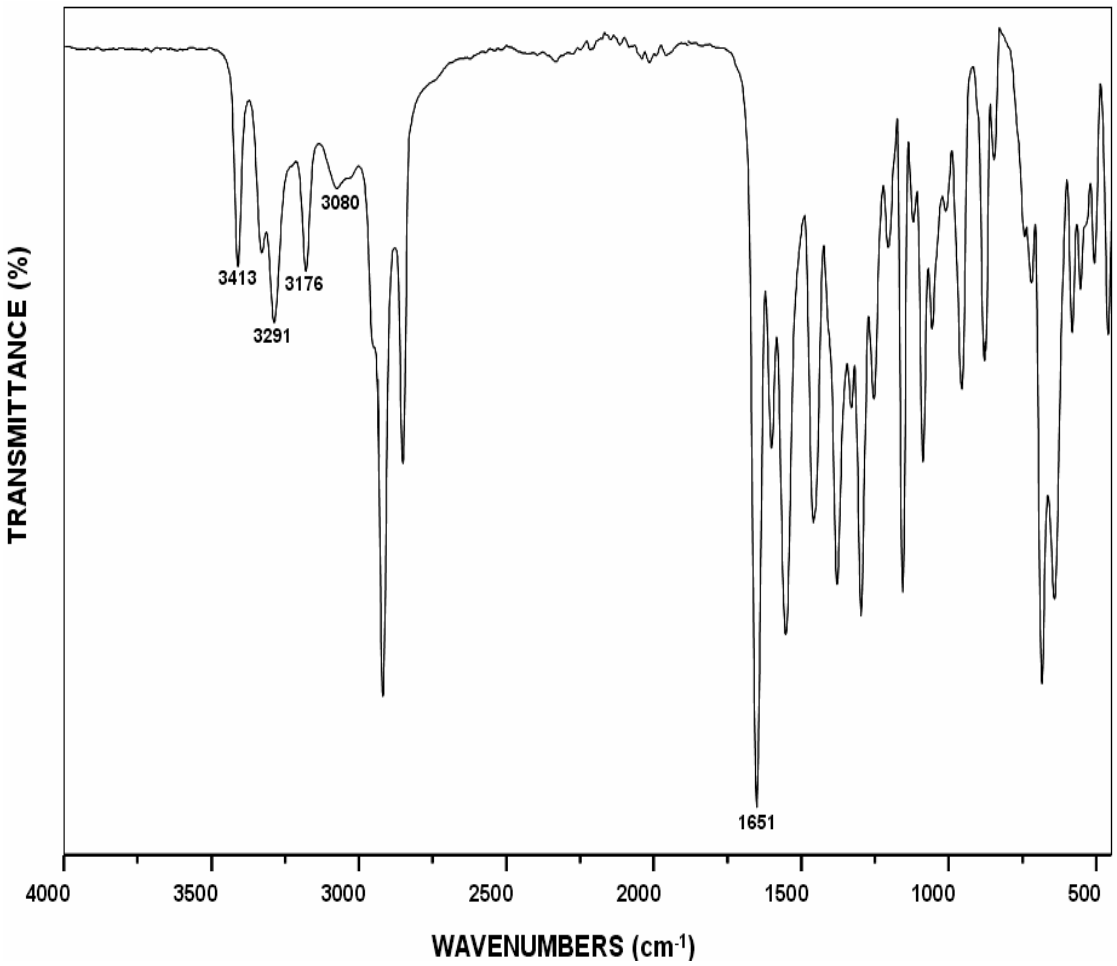

Figure 3.25 ATR spectrum of the C12GluDiamide/Mes-SO2-Asn-OH salt molecule.

3.1.8.2 NMR Analysis

NMR spectrum of the the C12GluDiamide/Mes-SO2-Asn-OH salt is on the Figure 3.26. We can see the peaks belong to the hydrocarbon chains, amino acids and aromatic protons around 1 ppm, between 2-4 ppm and 7 ppm respectively.

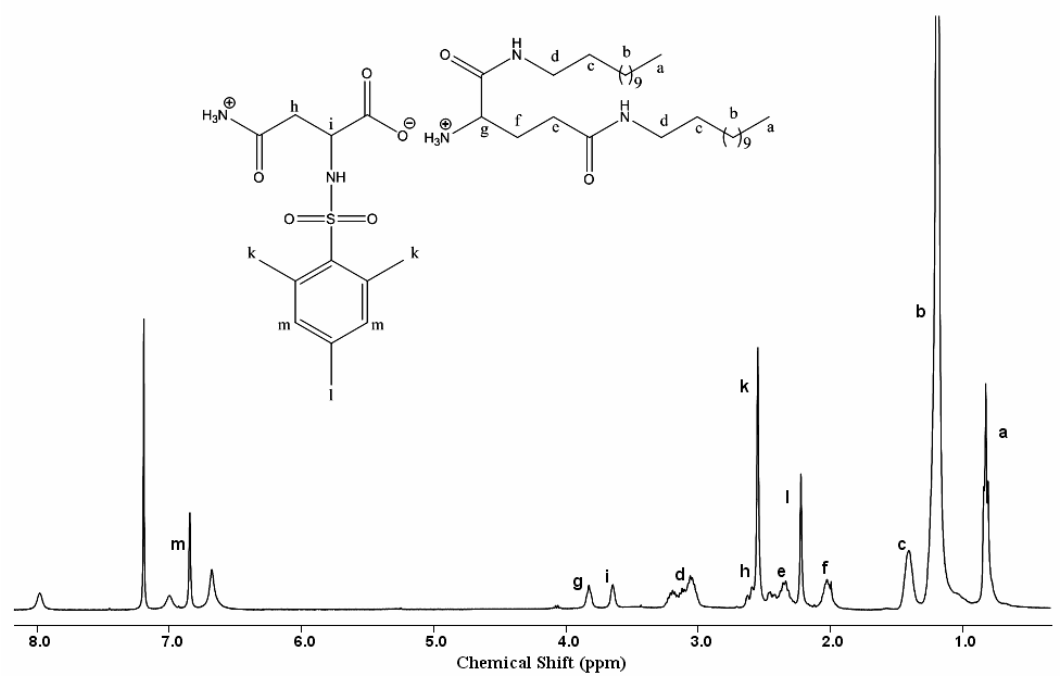

Figure 3.26 ^{1}H NMR spectrum of the C12GluDiamide/Mes-SO2-Asn-OH salt molecule.

3.1.8.3 POM Analysis

The POM observation of the sample was done at room temperature. The observed structure was a crystal. There are a lot of transparent, small pieces.

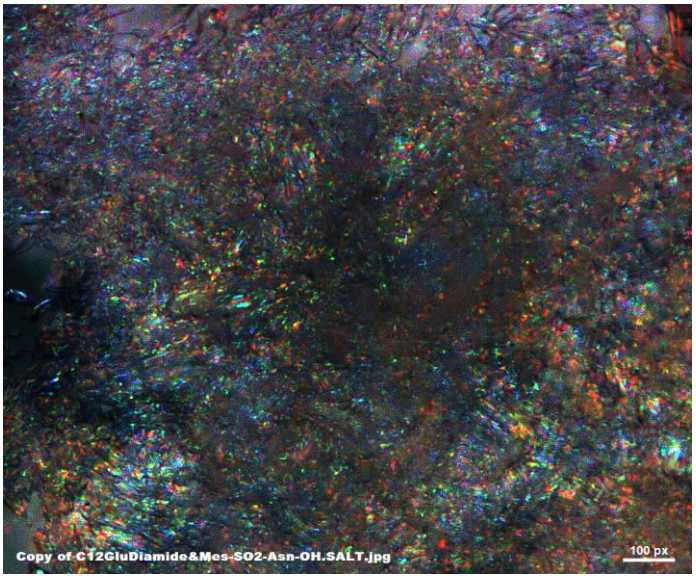

Figure 3.27 POM image of the C12GluDiamide/Mes-SO2-Asn-OH salt.

3.1.8.4 SEM Analysis

In comparison to C12GluDiamide/Mes-SO_2-Asn-OH salt with C12GluDiamide amphiphilic molecule, two photographs will be seen to bear some similarities. In this image, we can see there are some micro-sized ribbons which are mostly look like rod-like micelles in the C12GluDiamide's SEM image. And other important thing is aggregation of these micro-sized ribbons as can be seen in the second image. This aggregation may have probably occured due to π-π attraction of molecule's aromatic group or other supramolecular attraction like hydrogen bond, van der waals attraction etc. As observed in the first SEM picture of the amphiphilic molecule, the micro-sized ribbons are flexible and their widths are approximately 0.5μm.

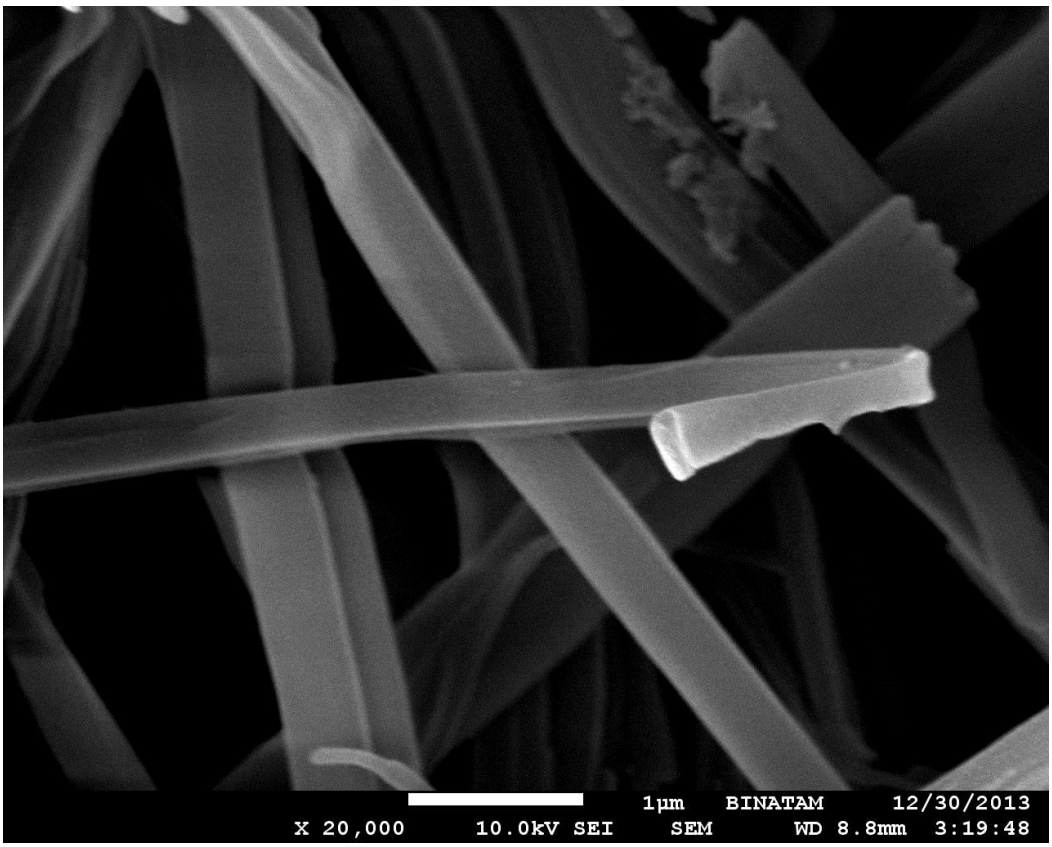

Figure 3.28 SEM image of the C12GluDiamide/Mes-SO2-Asn-OH salt.

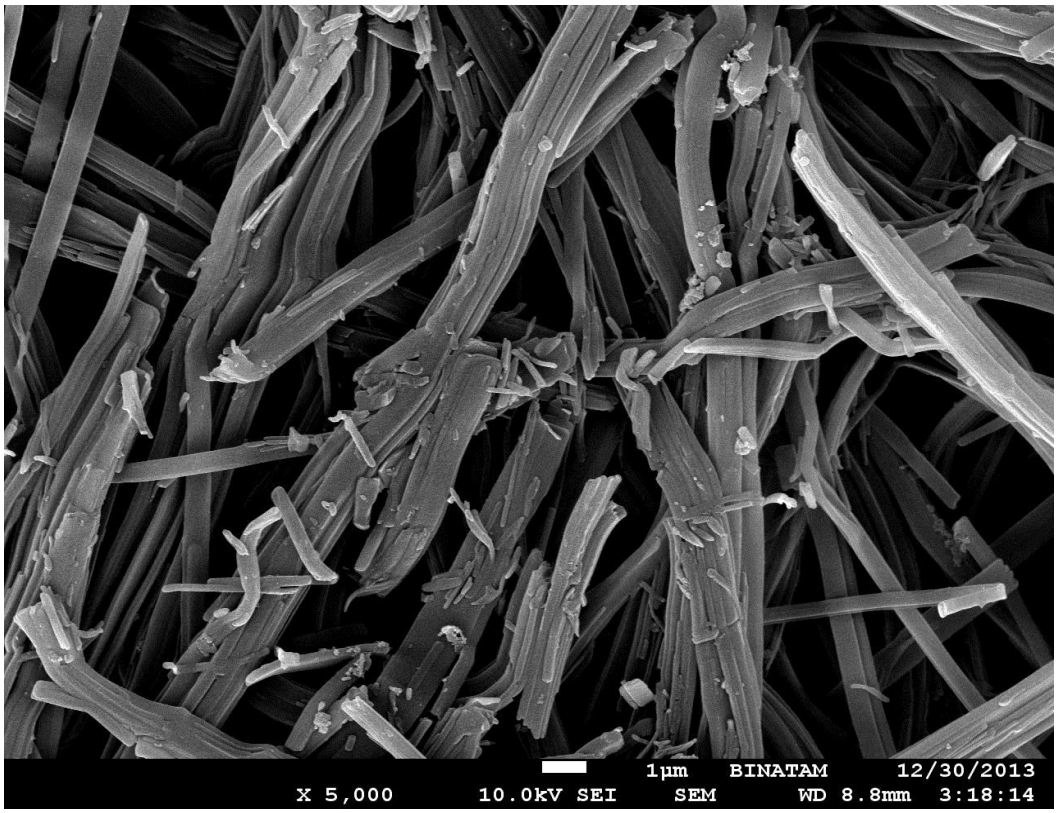

Figure 3.29 SEM image of the C12GluDiamide/Mes-SO2-Asn-OH salt.

3.1.8.5 The Structure of Optimized C12GluDiamide/Mes-SO_2-Asn-OH Salt

Optimized structure of C12GluDiamide/Mes-SO_2-Asn-OH Salt can be seen on the Figure 3.30. The calculated packing parameter for the C12GluDiamide/Mes-SO_2-Asn-OH Salt is 0.42, because of the big head group of the molecule. This value is within the cone molecular shape according to the packing parameter table, but as we can see, the molecules's shape seems to be more likely truncated cone. Because the molecule has two hydrocarbon chains and the packing parameter value close to the 0.5, we believe that truncated cone shape would be more convenient to obtain more accurate results. Accordingly, we can say the aggregation behavior of the molecule can be flexible lamellar or vesicle. The thickness of the micro-sized ribbons seems uncertainly. It is about 100nm and if we consider the one amphiphilic molecule's length is about 3nm, there must be at least 88nm hole in the micro-sized ribbons. This also supports that the aggregation type of the molecule is flexible ribbon like vesicle, such as long suppressed drug capsule.

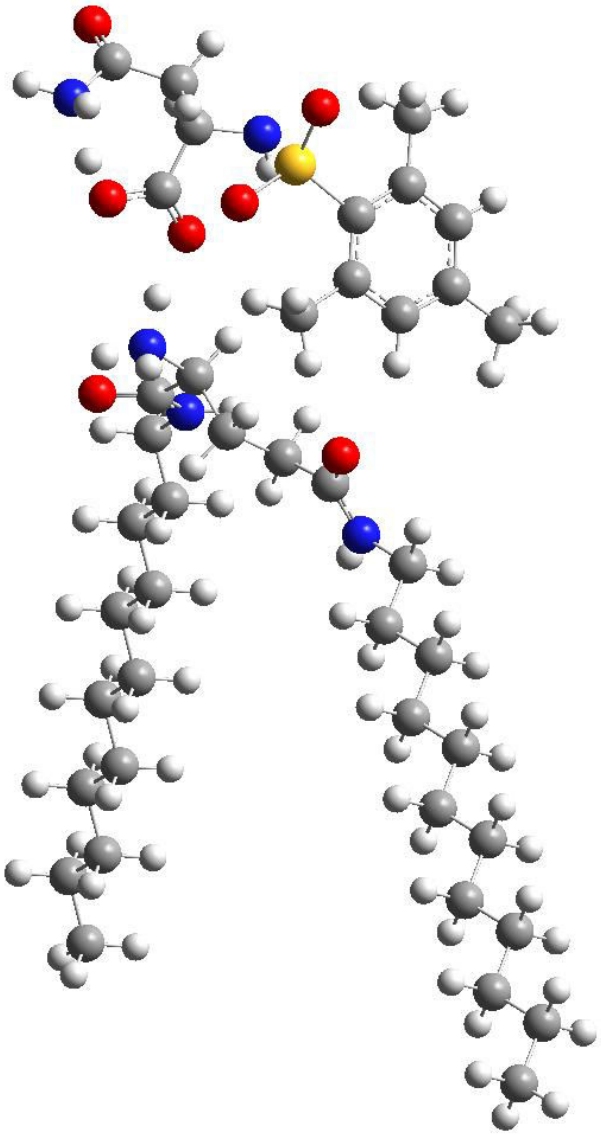

Figure 3.30 Optimized structure of C12GluDiamide/Mes-SO_2-Asn-OH Salt.

3.1.8.6 Surface Tension of C12GluDiamide/Mes-SO2-Asn-OH Salt

The surface tension measure was done using 0.01M solution of the C12GluDiamide/Mes-SO2-Asn-OH Salt and the critical micelle concentration of the substance was found 0.00005M.

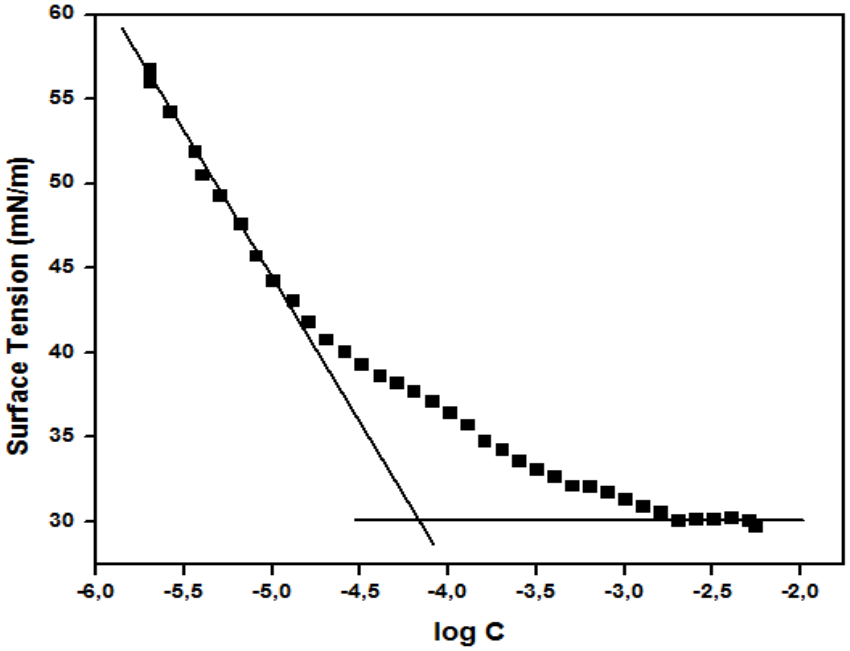

Figure 3.31 Surface tension vs. log concentration curves for the C12GluDiamide/Mes-SO_2-Asn-OH Salt.

Table 3.3 The surface tension values of C12GluDiamide/Mes-SO_2-Asn-OH Salt.

	CAC ($Mol.L^{-1}$)	$\gamma_{minimum}$ ($mN.m^{-1}$)	Γ ($mol.cm^{-2}$)	σ(wilhelmy) ($Å^2$/molecule)	σ(theoretical) ($Å^2$/molecule)
C12GluDiamide/ Mes-SO_2-Asn-OH Salt	$6,3.10^{-5}$	29,7	$3,68.10^{-10}$	451	117

CHAPTER 4

CONCLUSION

In this thesis study, amino acid based double chained cationic amphiphiles were synthesized depending on their bond type and amino acids. We could have the opportunity to compare the amphiphiles depending on the bond type, but not the amino acids. According to the results obtained, we observed the experimental and theoretical results are compatible. We compared effect of the amide and ester bonds on the aggregation type using glutamic acid double chained surfactant. Because the lone pair of electrons on the nitrogen in amide is delocalized into the carbonyl, amide bond is rigid and planar, so it does not allow to the movement of double chains of the molecule as far as containing ester bond. Ester bond is not delocalized into the carbonyl and it is more free than that the including amide bond. With this difference, we observed theoretically calculated packing parameter of the C12GluDiester is lower than the C12GluDiamide. We also observed these theoretical results are compatible with the experimental results and, while the aggregation type of the C12GluDiester is flexible lamellar, the aggregation of the C12GluDiamide is hexagonal in accordance with their molecular shapes. During the experiments we also noticed of gel formation of the C12GluDiamide even at low concentrations. This is also very valuable information for us and it can be used for further studied.

For the purpose of drug delivery, we tried to connect Mes-SO_2-Asn-OH molecule to our double chained cationic surfactants electrostatically. We could obtain the salt form of Mes-SO_2-Asn-OH molecule with C12GluDiamide, but not the C12GluDiester. We also tried to connect the salt form of the C12GluDiester with Boc-b-Ala and salicylic acid, but we could not get the positive results and we concluded that an attraction between two ester bonds and cationic NH_3 group may cause this. Binding a molecule on the C12GluDiamide amphiphilic

molecule did not change the aggregation of the C12GluDiamide greatly and hexagonal vesicle type aggregation could obtain in both amphiphiles, tubules for the C12GluDiamide and suppressed drug capsule like micro-sized ribbon for the C12GluDiamide/Mes- SO_2-Asn-OH salt. These are good aggregation types for the drug delivery system and we saw the calculated packing parameter is also compatible with experimental results for the C12GluDiamide/Mes-SO_2-Asn-OH salt.

We also made surface tension measurement of the amphiphilic molecules and observed that they have lower critical aggregation concentration than some similar surfactants molecules in the literature. Using the critical aggregation concentration results we calculate the experimental head group area of the amphiphilic molecules. When we compared experimental head group area of the molecules with the theoretical head group area, we found the experimental results are four times larger than theoretical results. Actually, we cannot think the amphiphilic molecules adjacent each other in water. There must be a distance between the amphiphilic molecules. This can be due to several factors such as hydrogen bonding, van der waals attractions, water molecules etc.

REFERENCES

[1] Pinazo, A., et al., "Aggregation Behavior in Water of Monomeric and Gemini Cationic Surfactants Derived from Arginine''. *Langmuir*, Vol. 15(9): pp. 3134-3142, 1999.

[2] Landsmann, S., C. Lizandara-Pueyo, and S. Polarz, "A New Class of Surfactants with Multinuclear, Inorganic Head Groups''. *Journal of the American Chemical Society*, Vol 132(14): pp. 5315-5321, 2010.

[3] Maiti, P.K., et al., "Self-Assembly in Surfactant Oligomers: A Coarse-Grained Description through Molecular Dynamics Simulations''. *Langmuir*, Vol 18(5): pp. 1908-1918, 2002.

[4] Salager, J.-L., *Surfactants Types and Uses*, 2002, http://www.nanoparticles.org/pdf/Salager-E300A.pdf

[5] Zhao, X., "Design of self-assembling surfactant-like peptides and their applications''. *Current Opinion in Colloid & Interface Science*, Vol 14(5): pp. 340-348, 2009.

[6] Myers, D., "The Organic Chemistry of Surfactants, in Surfactant Science and Technology''. *John Wiley & Sons*, Inc. pp. 29-79, 2005.

[7] Porter, M.R., "Handbook of Surfactants''. 2nd ed. *Blackie Academic and Professional*. London, U.K., 1994.

[8] Hugo, W.B.R., A. D., "Principles and practice of disinfection. In Types of Antimicrobial Agents''. 2nd ed. *Blackwell Scientific Publications*, ed. A.D. Russel, Hugo,W. B., Ayliffe, G. A. J. Oxford, U.K. 1992.

[9] Ilies, M.A., et al., "Lipophilic Pyrylium Salts in the Synthesis of Efficient Pyridinium-Based Cationic Lipids, Gemini Surfactants, and Lipophilic Oligomers for Gene Delivery''. *Journal of Medicinal Chemistry*. Vol 49(13): pp. 3872-3887, 2006.

[10] Vyas, S.M., et al., "Synthesis and biocompatibility evaluation of partially fluorinated pyridinium bromides''. *New Journal of Chemistry*. Vol 30(6): pp. 944-951, 2006.

[11] Heyes, J.A., et al., “Synthesis of Novel Cationic Lipids: Effect of Structural Modification on the Efficiency of Gene Transfer’’. *Journal of Medicinal Chemistry*, Vol 45(1): pp. 99-114, 2001.

[12] Stephenson, B.C., et al., “Experimental and Theoretical Investigation of the Micellar-Assisted Solubilization of Ibuprofen in Aqueous Media’’. *Langmuir*, Vol 22(4): pp. 1514-1525, 2006.

[13] Bramer, T., N. Dew, and K. Edsman, “Pharmaceutical applications for catanionic mixtures’’. *Journal of Pharmacy and Pharmacology*, Vol 59(10): pp. 1319-1334, 2007.

[14] Wang, W., W. Lu, and L. Jiang, “Influence of pH on the Aggregation Morphology of a Novel Surfactant with Single Hydrocarbon Chain and Multi-Amine Headgroups’’. *The Journal of Physical Chemistry B*, Vol 112(5): pp. 1409-1413, 2008.

[15] Mezei, A., et al., “Self assembly of pH-sensitive cationic lysine based surfactants’’. *Langmuir*, Vol 28(49): pp. 16761-71, 2012.

[16] Paulsson, M. and K. Edsman, “Controlled Drug Release from Gels Using Surfactant Aggregates. II. Vesicles Formed from Mixtures of Amphiphilic Drugs and Oppositely Charged Surfactants’’. *Pharmaceutical Research*, Vol 18(11): pp. 1586-1592, 2001.

[17] Nogueira, D.R., et al., “Phospholipid bilayer-perturbing properties underlying lysis induced by pH-sensitive cationic lysine-based surfactants in biomembranes’’. *Langmuir*, Vol 28(32): pp. 11687-98, 2012.

[18] Brito, R.O., et al., “Enhanced interfacial properties of novel amino acid-derived surfactants: Effects of headgroup chemistry and of alkyl chain length and unsaturation’’. *Colloids Surf B Biointerfaces*, Vol 86(1): pp. 65-70, 2011.

[19] Pinazo, A., et al., “Amino Acids as Raw Material for Biocompatible Surfactants’’. *Industrial & Engineering Chemistry Research*, Vol 50(9): pp. 4805-4817, 2011.

[20] Li, Y., “*Synthesis and physicochemical study of novel amino acid based surfactants’’*, M.S. Thesis, Chalmers University of Technology, 2011.

[21] Moran, C., et al., “Amino Acids, Lactic Acid and Ascorbic Acid as Raw Materials for Biocompatible Surfactants, in Surfactants from Renewable Resources’’. *John Wiley & Sons, Ltd*. pp. 85-107, 2010.

[22] Myers, D., “Fluid Surfaces And Interfaces, in Surfactant Science and Technology’’. *John Wiley & Sons, Inc*. pp. 94-120, 2005.

[23] Nagarajan, R., “Molecular Packing Parameter and Surfactant Self-Assembly: The Neglected Role of the Surfactant Tail’’. *Langmuir*, Vol 18(1): pp. 31-38, 2001.

[24] Pasquali, R.C., M.P. Taurozzi, and C. Bregni, "Some considerations about the hydrophilic-lipophilic balance system''. *Int J Pharm*. Vol 356(1-2): pp. 44-51, 2008.

[25] Zhang, R. and P. Somasundaran, "Aggregate Formation of Binary Nonionic Surfactant Mixtures on Hydrophilic Surfaces''. *Langmuir*, Vol 21(11): pp. 4868-4873, 2005.

[26] Zhai, L., "Salt-Induced Vesicle Formation from Single Anionic Surfactant SDBS and Its Mixture with LSB in Aqueous Solution''. *The Journal of Physical Chemistry B*. Vol 109(12): pp. 5627-5630, 2005.

[27] Liu, M., et al., "Preparation, characterization and properties of liposome-loaded polycaprolactone microspheres as a drug delivery system''. *Colloids and Surfaces A: Physicochemical and Engineering Aspects*. Vol 395(0): pp. 131-136, 2012.

[28] Wang, B., Siahaan, T., Soltero, R., "Drug Delivery: Principles and Applications, Frontmatter, in Drug Delivery'', *John Wiley & Sons, Inc*. pp. i-xi, 2005.

[29] Yoo, J.-W., N. Doshi, and S. Mitragotri, "Adaptive micro and nanoparticles: Temporal control over carrier properties to facilitate drug delivery''. *Advanced Drug Delivery Reviews*. Vol 63(14–15): pp. 1247-1256, 2011.

[30] Nill, B., "*Liposomes for Drug Delivery: from Physico-chemical Studies to Applications''*, Uppsala. pp. 71, 2003.

[31] Brito, R.O., "Self-Assembly in a Catanionic Mixture with an Aminoacid-Derived Surfactant: From Mixed Micelles to Spontaneous Vesicles*''. The Journal of Physical Chemistry B.* Vol 110(37): pp. 18158-18165, 2006.